COPY NO. 3

TM X-62,131
SSPD-99
Copy No.____

S P A C E S H U T T L E T E C H N O L O G Y
P R E L I M I N A R Y D A T A

AN INVESTIGATION OF THE FEASIBILITY OF SIMULATING GASEOUS EXHAUST PLUMES WITH SOLID BODIES IN SONIC BOOM STUDIES

by

Raymond M. Hicks
and Joel P. Mendoza

This document should be
referenced as NASA TM X-62,131

August 17, 1973

NASA LIBRARY
AMES RESEARCH CENTER
MOFFETT FIELD, CALIF.

Ames Research Center
Moffett Field, California
94035

NATIONAL AERONAUTICS AND SPACE ADMINISTRATION

AN INVESTIGATION OF THE FEASIBILITY OF SIMULATING GASEOUS EXHAUST PLUMES WITH SOLID BODIES IN SONIC BOOM STUDIES

Raymond M. Hicks and Joel P. Mendoza
Ames Research Center

ABSTRACT

A study was undertaken to determine the size (radius distribution and length) of solid bodies required to simulate the sonic boom overpressures produced by cold-flow exhaust plumes generated by ejecting nitrogen gas through an annular nozzle at the base of a cone-cylinder model.

Pressure signatures measured for both nitrogen gas and solid body plumes have shown that the radius distribution of the solid body should be slightly smaller than the mixing boundary of the gaseous plume; and that the length of the solid body plume must be increased with increasing Mach number to obtain good correlation of the sonic boom created by the nitrogen plume with the sonic boom created by the solid body plume.

AN INVESTIGATION OF THE FEASIBILITY OF SIMULATING GASEOUS EXHAUST PLUMES WITH SOLID BODIES IN SONIC BOOM STUDIES

Raymond M. Hicks and Joel P. Mendoza
Ames Research Center

SUMMARY

An investigation was conducted to determine the radius distribution and length of a solid body required for accurate simulation of the sonic boom overpressures produced by cold flow exhaust plumes generated by ejecting gas through an annular nozzle at the base of a cone-cylinder model. High pressure nitrogen gas was used to generate the plumes at test Mach numbers of 2.94 and 3.92. The model chamber pressure and wind tunnel total pressure were adjusted to produce plume diameters at least three times the maximum model diameter at one model length from the base of the cone-cylinder.

Pressure signatures measured for both the nitrogen gas and solid body plumes have shown that the radius distribution of the solid body should be slightly smaller than the mixing boundary of the gaseous plume; and that the length of the solid body plume must be long enough to prevent the expansion from the plume base from affecting the positive portion of the pressure signature. Furthermore, it was found that the length required increases with increasing Mach number.

NOTATION

h	distance from model axis to static probe or flat plate, m.
l	model reference length, m (see figure 1)
M	Mach number
p	reference pressure, cm-Hg
p_c	model chamber pressure, cm-Hg
p_t	total pressure, cm-Hg
r	exhaust plume radius, cm.
y	distance along axis of plume, cm
Δp	sonic boom overpressure, cm-Hg
Δx	distance along abscissa of pressure signature, m.

INTRODUCTION

For several years an effort has been underway to develop methods for predicting the sonic boom overpressure created by aircraft with and without large exhaust plumes maneuvering at hypersonic Mach numbers. The technique for predicting the ground overpressure consists of extrapolating near field wind tunnel pressure signatures to the far field by the method of reference 1. The procedure has been thoroughly evaluated for vehicles without exhaust plumes through comparisions of estimates based on wind-tunnel data with measurements made during the reentry phases of the Apollo 15 and 16 missions (references 2 and 3). These comparisons have shown that accurate predictions of ground overpressure can be made over a Mach number range from 1.16 to 9.71 for aircraft without exhaust plumes. However, unpublished comparisons of predictions and measurements for the launch phases of the Apollo 15, 16 and 17 missions, where the exhaust plume is the major contributor to the ground overpressure, have been less than satisfactory. For some flight conditions good agreement between predicted and measured overpressure has been obtained while at others the agreement has been poor. The inconsistency in results has been found to be related to incorrect simulation of the exhaust plume by the use of solid bodies in wind-tunnel tests. The incorrect simulation is due to a lack of information as to which plume boundary and what length the solid body should have. Simulations based on both the theoretical mixing boundary and the theoretical inviscid boundary with lengths varying from 1/2 to 2-1/2 model lengths have been tried without consistent success. Because of this problem an investigation was undertaken to compare pressure signatures generated by a model having a nitrogen gas exhaust plume with signatures generated by the same model but with the gas plumes simulated by solid bodies. Results of the study are reported herein.

MODEL, APPARATUS AND TEST CONDITIONS

A detailed drawing of the cone-cylinder model used in the exhaust plume study is shown in figure 1. High pressure nitrogen gas was supplied to the model through the sting as indicated in the figure. The wind tunnel nitrogen supply was connected to the sting with a flexible line. This permitted the model and sting to be traversed fore and aft through a distance of 76.2cm (30 in.) in the wind tunnel for the purpose of acquiring the pressure signatures. The model was designed and fabricated by personnel of the Jet Propulsion Laboratory (JPL). The material used was aluminum.

Pressure signatures generated by the model with nitrogen plumes were measured by a 2-degree (included angle) conical static-pressure probe connected to a 5.17-cm-Hg (1 psi) capacitance-type pressure transducer mounted outside the tunnel and by a Kulite transducer flush-mounted in a flat plate (see the installation photographs of figure 2). Pressure signatures generated by the model alone and with simulated solid body plumes were measured by the static-pressure probe only. The Kulite transducer has an active diaphragm diameter of 0.318-cm (0.125 in), a full-scale capacity of 129.25-cm-Hg (25 psi), a flat frequency response to 50 KHz and a natural frequency in excess of 125 KHz. The distance from the center-line of the model to the static pressure probe was identical to the distance from the center-line of the model to the upper surface of the flat plate. This allowed direct comparisons of the pressure signatures measured by each device with only a correction for reflection factor. The purpose of using the Kulite transducer was to measure the fluctuations in the flow field created by the plumes.

The test was conducted in the JPL 20-inch supersonic wind tunnel at free stream Mach numbers of 2.94 and 3.92. The total pressure was 30-cm-Hg (5.8 psi) at Mach 2.94 and 50-cm-Hg (9.67 psi) at Mach 3.92. These total pressures combined with chamber pressures of 3361-cm-Hg (650 psi) at Mach 2.94 and 3102-cm-Hg (600 psi) at Mach 3.92 produced the desired sizes of the nitrogen gas plumes.

RESULTS AND DISCUSSION

Schlieren and shadowgraph pictures of the cone-cylinder model with and without nitrogen plumes are shown in figures 3 and 4, respectively. The schlieren pictures give a good view of the external flow around the exhaust plumes whereas the shadowgraph pictures give a better indication of the flow in the mixing region between the plume flow and the external flow. Coordinates measured on the schlieren and shadowgraph pictures were used to size the solid bodies that were used to simulate the nitrogen plumes. Solid bodies were made to the dimensions of both the inner shock and mixing boundaries of the gaseous plumes. The inner shock is clearly visible on both the schlieren and shadowgraph pictures whereas the extent and structure of the mixing boundary is more clearly delineated on the shadowgraph pictures.

Graphs of the coordinates used to size the solid body plumes are shown in figure 5. The mixing boundary and inner shock are shown for both Mach numbers. The dashed line is a fairing of the turbulent mixing boundary shown in figure 4. The simulated plumes were truncated one model length from the model base because of wind tunnel blockage limitations. This plume length proved to be inadequate for good plume simulation as discussed later. Photographs of each of the solid body plumes installed behind the cone-cylinder model are shown in figure 6.

Wind tunnel pressure signatures recorded during testing of the model with and without nitrogen gas and solid body exhaust plumes are shown in figure 7. It was not possible to obtain full signatures for the model either with the gaseous or solid body plumes because of the limited travel of the linear actuator used to vary the longitudinal position of the model in the test section. However, the full signature is not usually required since the parameter of primary importance to most investigations is the maximum overpressure along the groundtrack which can be calculated from just the positive portion of the wind tunnel signature. Hence, the use of solid body plumes which duplicated the entire flow field of the nitrogen plumes was considered beyond the scope of the present study. Summary plots comparing pressure signatures generated by the model with exhaust plumes simulated both by the nitrogen gas and the solid bodies are presented in figure 8. The following facts are apparent from results shown in the figure. First, at both Mach numbers, the solid-body plume sized according to the dimensions of the inner shock in the nitrogen plume produced peak flow field pressures well below those generated by the nitrogen plume itself. Second, the pressure signature generated by the solid-body plume sized according to the dimensions of the mixing boundary observed with the nitrogen plume agrees reasonably well with the signature generated by the nitrogen plume at least to the point where the expansion from the plume base is encountered. Finally, the expansion of the flow at the base of the mixing boundary plume produces a discontinuity in the slope of the pressure signature behind the point of maximum overpressure with an attendant decrease in positive area of the signature. This discontinuity affects the critical positive area of the signature only for the plume based on mixing boundary dimensions. As the Mach number is increased the point of discontinuity in slope of the pressure curve for the mixing boundary plume is observed to move toward the peak overpressure thereby increasing the effect on the positive area of the signature.

The discontinuities in slope observed for the mixing boundary plume would not appear if the wind tunnel signatures had been measured at a greater distance from the model since the plume shock and expansion fan from the plume base tend to coalesce at a distance away from the model (figures 9(b) and 9(d)). Hence, it is important that wind tunnel signatures for models with exhaust plumes simulated with solid bodies be obtained close to the model so that plume base effects can be detected and the plume length increased, if necessary. It is clear that the length of the solid body used to simulate a gaseous plume must be increased as Mach number is increased and its radial dimensions should be slightly smaller than the mixing boundary of the gaseous plume. This is particularly important information since the mixing boundary is a quantity calculated with some theories in current use. However, further effort is needed to establish scale factors for any Mach number and altitude by which the theoretical mixing boundary can be multiplied by to give the radius distribution for constructing solid body simulated plumes for use in wind tunnel tests. Furthermore, any future effort should include a correlation of results with exhaust plumes simulated by both hot and cold flows. It should be emphasized that no attempt has been made during this study to simulate the exhaust plume of any existing or future rocket-powered vehicle but rather to investigate exhaust plume simulation in general.

Schlieren photographs of the flow fields generated by the model with the various simulated exhaust plumes for both test Mach numbers are shown in figure 9. A comparison of figures 9(b) and 9(d) graphically shows the decrease in distance due to increasing Mach number, that was discussed above in connection with the pressure signatures of figure 8, between the plume shock and the first expansion characteristic from the plume base. Again it is clear that the length of the plume simulated with solid bodies must be increased with increasing Mach number to delay the effect of the expansion from the artifically introduced plume base. Comparing results in figures 3(b) and 3(d) with results in figures 9(b) and 9(d) indicates that the model flow fields for the nitrogen and solid body mixing boundary plumes are quite similar until the expansion from the plume base is encountered. This tends to explain the similarities shown by the pressure signatures of figure 8 and to indicate that it may be possible to simulate real exhaust plumes by solid bodies for sonic boom testing.

Experiments conducted with exhaust plumes from full scale rocket motors have indicated that the pressure field generated external to the plume may be unsteady. Because of these results measurements were made to explore the consequences of not simulating the possibly unsteady flow generated by the nitrogen plumes with the more steady flows around the solid-body plumes in the present investigation.

The static pressure probe used to detect the flow field pressures was replaced by a fast-response transducer flush mounted in a flat plate located the same distance below the model center line as the static probe (see figure 2). Pressure traces taken at Mach 2.94 as the model with the nitrogen exhaust plume passed over the transducer were recorded by photographic oscilloscope traces for various model positions. Results for 5 values of $\Delta x/_{l}$ are shown in figure 10 (the location of the transducer in the model flow field at each position can be ascertained by correlating the positions indicated in the figure with the signature of figure 7(b)). The oscilloscope trace for $\Delta x/_{l} = 0.1$, shown in figure 10(a), was taken with the model retracted far enough downstream to ensure that an adequate "noise" level for the instrumentation and free stream turbulence could be established. Subsequent oscilloscope traces, shown in figures 10(b) through 10(e), were taken as the bow shock, plume shock and expansion behind the plume shock passed over the transducer. Note the increase in pressure fluctuation as the plume shock approaches the transducer (figure 10(c)). Apparently, the plume shock is unsteady and its intermittent effects are being felt through the boundary layer by the transducer when the model is positioned such that the plume shock is slightly upstream from the leading edge of the transducer. A small change in model position, from $\Delta x/_{l} = 0.79$ to $\Delta x/_{l} = 0.82$ (figure 10(c) and 10(d)), causes the mean pressure level to increase and the magnitude of the fluctuation to decrease. Apparently, the movement of the oscillating plume shock is confined entirely to the transducer when $\Delta x/_{l} = 0.82$. The amount of fluctuation in the expansion field behind the plume shock can be seen to be no greater than for the free stream (compare figures 10(a) and 10(e)).

A question which arose during the course of the investigation is:

Was the observed pressure fluctuation due to movement of the plume shock or was shock induced flow separation on the flat plate responsible for the fluctuation? Two steps were taken in an effort to answer this question because of its importance to the problem of plume simulation. First, high-speed moving pictures (5000 frames per second) of the flow field were taken. Analysis of the moving pictures revealed more movement of the plume shock than for other shock waves in the model flow field. The second step involved analysis of a schlieren photograph showing the impingement of the model-plume shock system on the flat plate. A close study of the schlieren photograph presented in figure 11 shows that both the bow shock and the plume shock cause boundary layer separation and since the oscilloscope trace of the bow shock pressures shows the same level of fluctuation as for the free stream while the fluctuations due to the plume shock are greater than for the free stream it can be concluded that the oscillation is not due to shock induced separation of the boundary layer.

From the evidence discussed above it can be concluded that the plume shock is unsteady. However, this does not preclude simulation of real rocket plumes by solid bodies for sonic boom studies. This can be deduced by comparing the average pressure levels from the oscilloscope records with the appropriate overpressures measured by the static pressure probe. Division of the average pressure level of figure 10(d) ($\Delta p/p \simeq 2.65$ by a reflection factor of 2.65 gives an overpressure value of approximately 1.0 which agrees well with the peak overpressure shown in figure 7(b). The reflection factor is 2.65 for this combination of shock strength and Mach number as discussed in the Appendix of reference 4. The bow shock strength from the trace shown in figure 10(b) ($\Delta p/p \simeq .65$) compares well with the bow shock strength shown in figure 7(b) ($\Delta p/p = .32$) when the former is divided by a reflection factor of 2.2 which is appropriate for the weaker strength bow shock (see reference 4).

CONCLUDING REMARKS

An experimental investigation has been conducted to determine the feasibility of simulating the effects of rocket exhaust plumes on near field pressure signatures of wind tunnel models by the use of "equivalent" solid body plumes. The results of the investigation have shown that solid body plumes can be used to simulate cold-flow nitrogem plumes if the radius distributions of the solid plumes are slightly less than the radius distributions of the mixing boundary of the nitrogen plumes and if the solid body plume is of suitable length. Further work is needed to establish the required length of solid body plume, for proper simulation, over a range of Mach numbers large enough to be applicable to most rocket powered vehicles operating within the Earth's atmosphere and to investigate the correspondence of effects due to hot-gas exhaust plumes with those created by cold-gas plumes of comparable size. Some additional effort is also needed to better assess the effects of the unsteadyness found in the flow fields around the nitrogen exhaust plumes.

REFERENCES

1. Thomas, Charles L.: Extrapolation of Sonic Boom Pressure Signatures by the Waveform Parameter Method. NASA TN D-6832, June 1972.

2. Hicks, Raymond M.; Mendoza, Joel P.; and Garcia, Frank Jr.: A Wind Tunnel-Flight Correlation of Apollo 15 Sonic Boom. NASA TM X-62,111, January 1972.

3. Garcia, Frank Jr.; Hicks, Raymond M.; and Mendoza, Joel P.: A Wind Tunnel-Flight Correlation of Apollo 16 Sonic Boom. NASA TM X-62,073, February 1973.

4. Hicks, Raymond M.; Mendoza, Joel P.; and Thomas, Charles L.: Pressure Signatures for the Apollo Command Module and the Saturn V Launch Vehicle with a Discussion of Strong Shock Extrapolation Procedures. NASA TM X-62,117, April 1972.

Note: All dimensions are
in meters (inches)

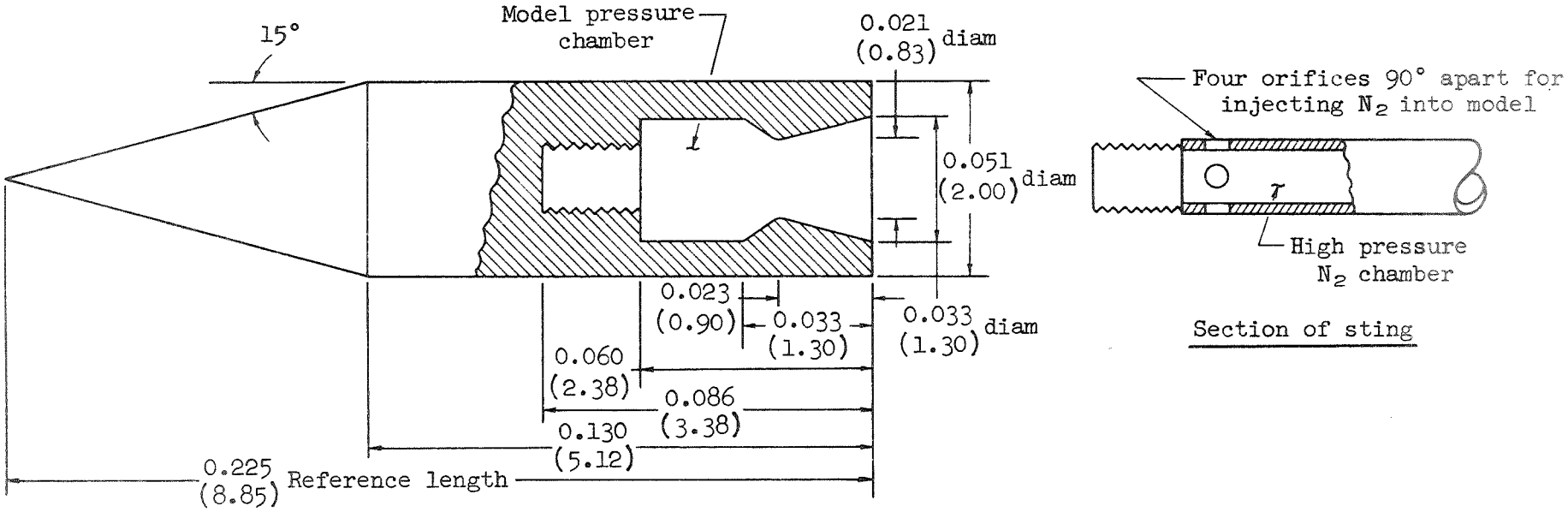

Figure 1.- Cone-cylinder model with exhaust nozzle.

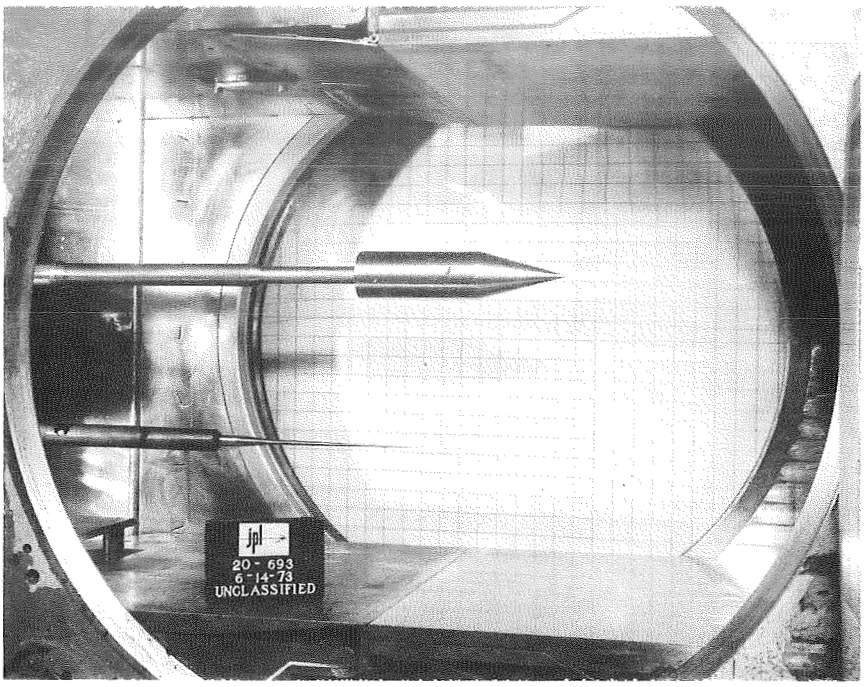

(a) Model and static pressure probe.

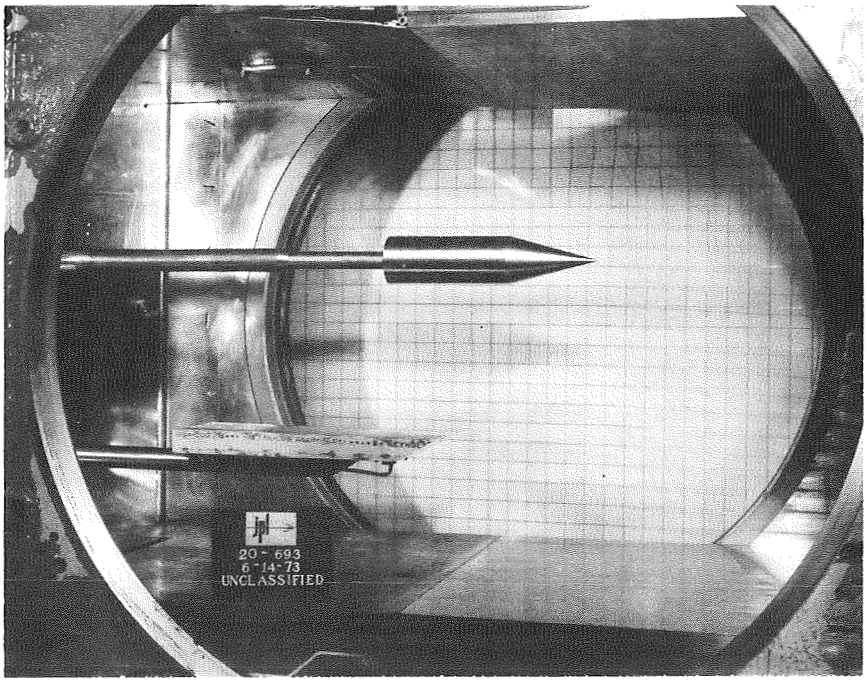

(b) Model and flat plate housing fast-response pressure transducer.

Figure 2.- Installation photograph.

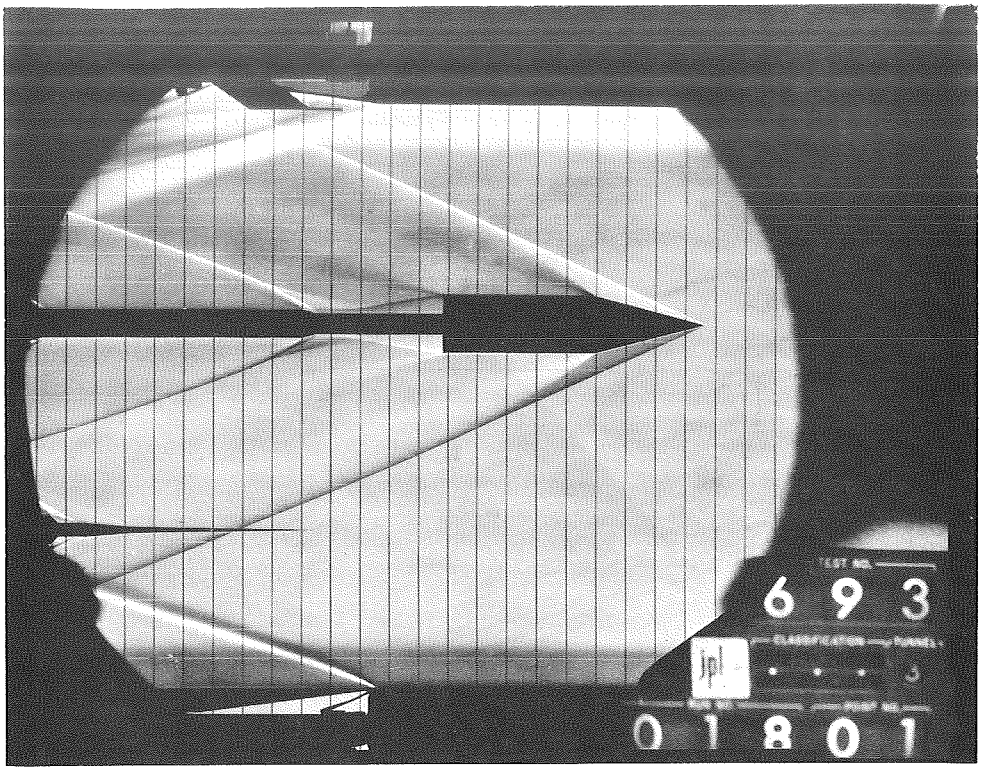

(a) Nitrogen off; M = 2.94, p_t = 30 cm-Hg.

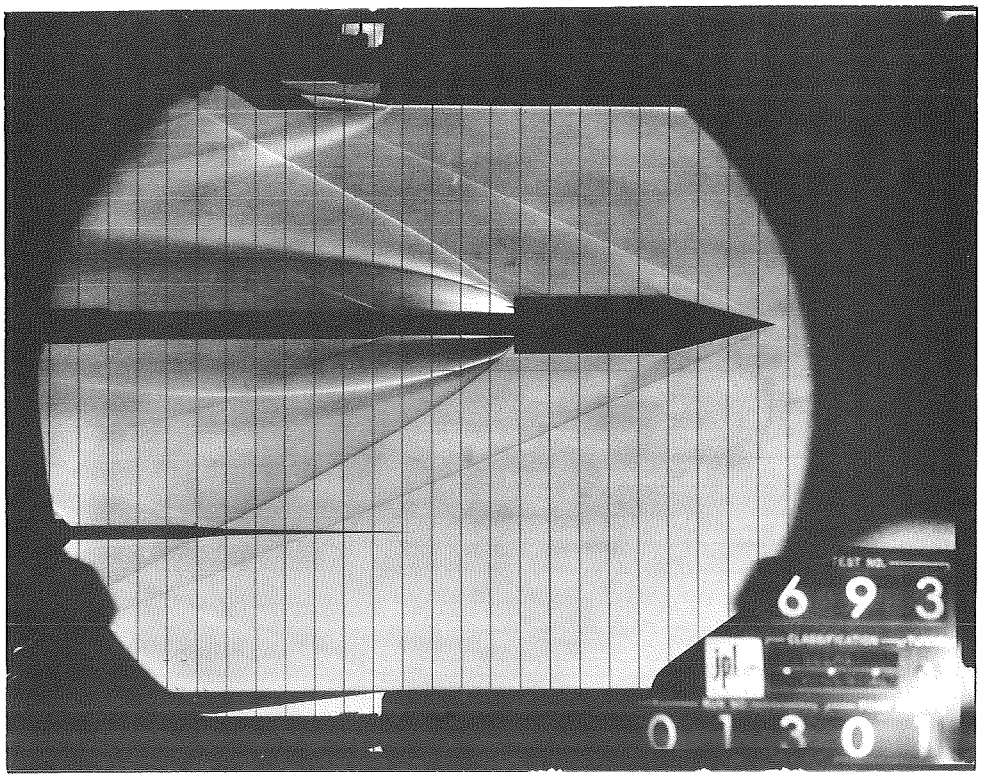

(b) Nitrogen on; M = 2.94, p_t = 30 cm-Hg, p_c = 3361 cm-Hg.

Figure 3.- Schlieren photographs of cone-cylinder model with and without nitrogen plume.

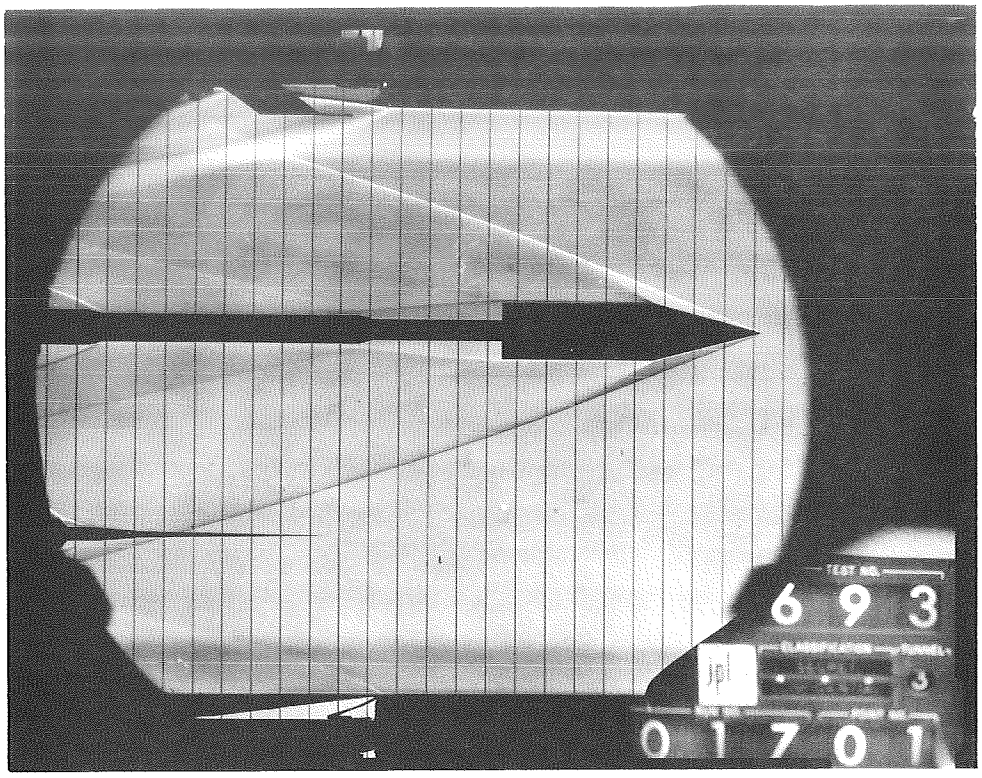

(c) Nitrogen off; M = 3.92, p_t = 50 cm-Hg.

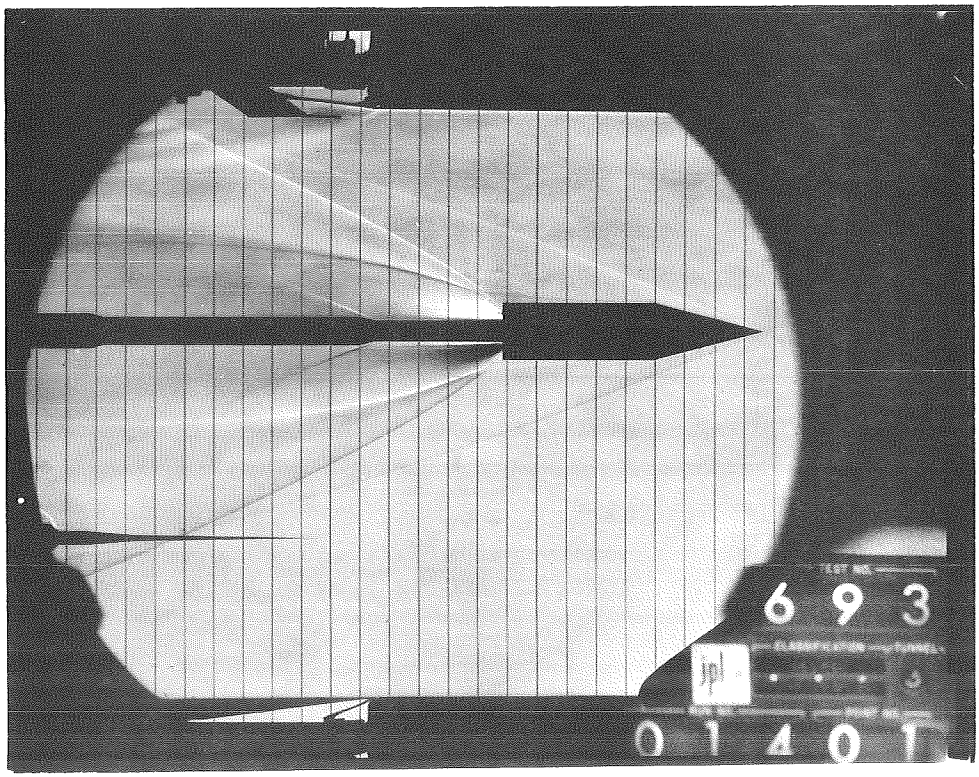

(d) Nitrogen on; M = 3.92, p_t = 50 cm-Hg, p_c = 3102 cm-Hg.

Figure 3.- Concluded.

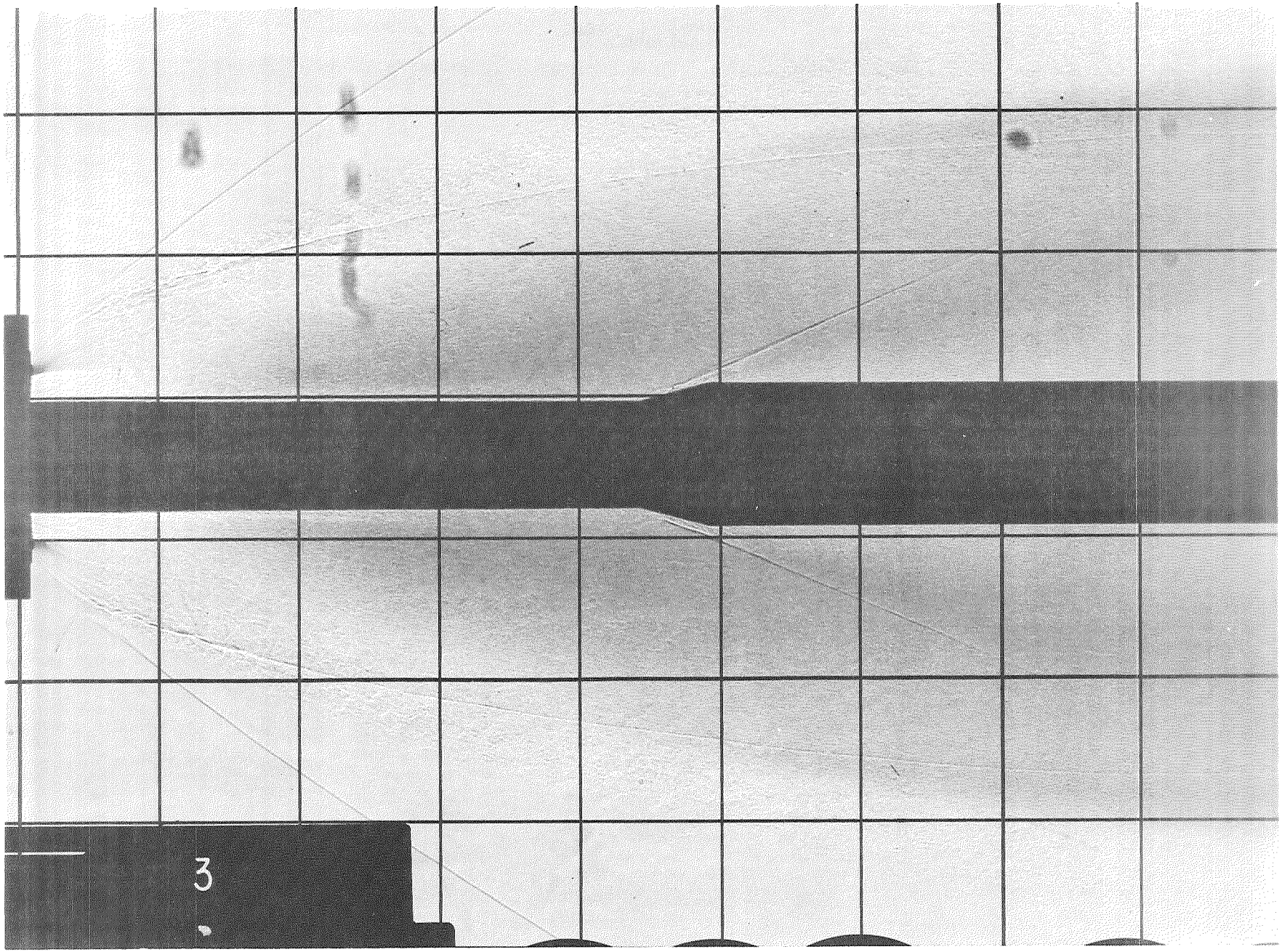

(a) M = 2.94, p_t = 30 cm-Hg, p_c = 3361 cm-Hg.

Figure 4.- Shadowgraph pictures of cone-cylinder model with nitrogen plumes.

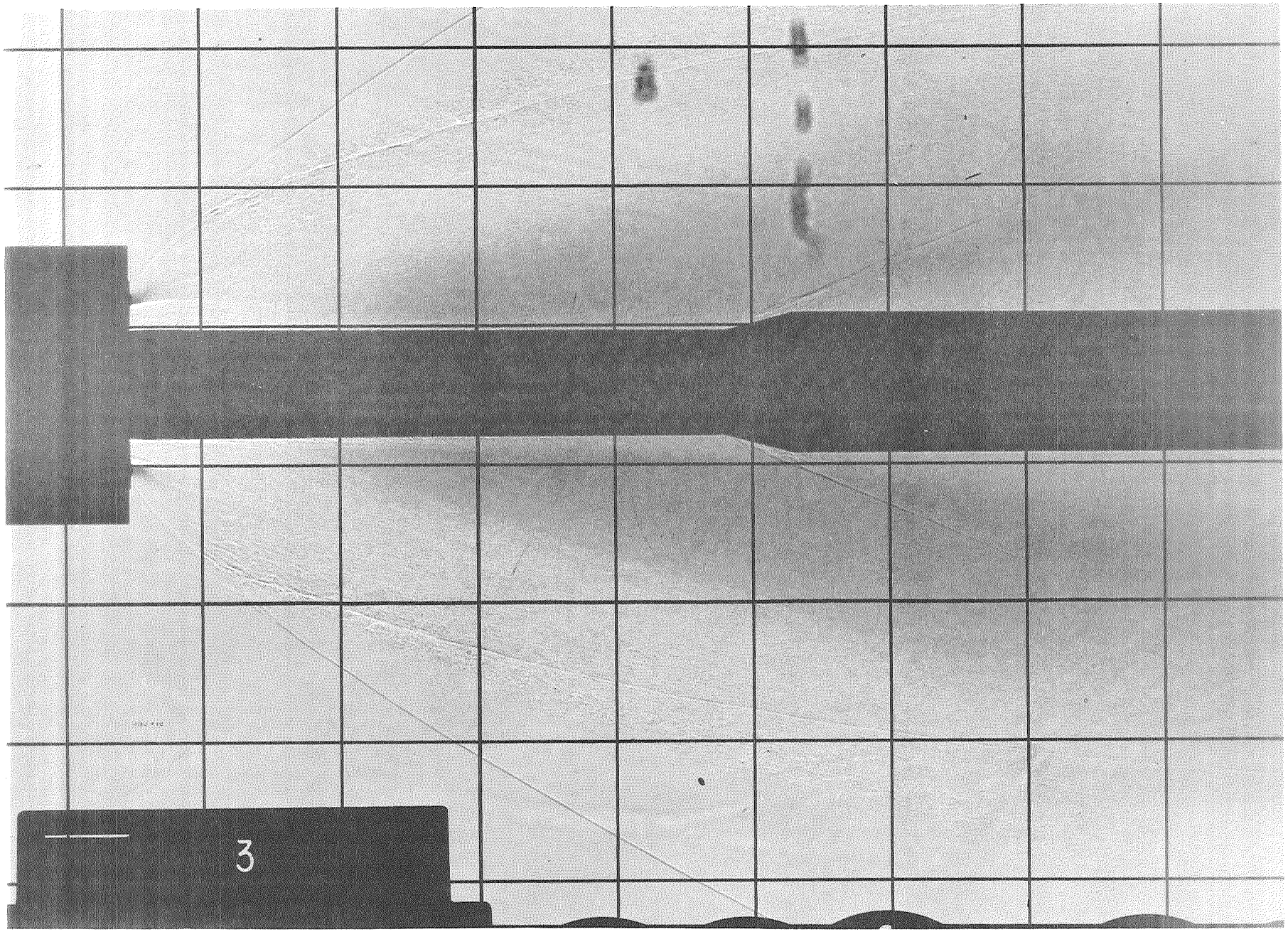

(b) M = 3.92, p_t = 50 cm-Hg, p_c = 3102 cm-Hg.

Figure 4.- Concluded.

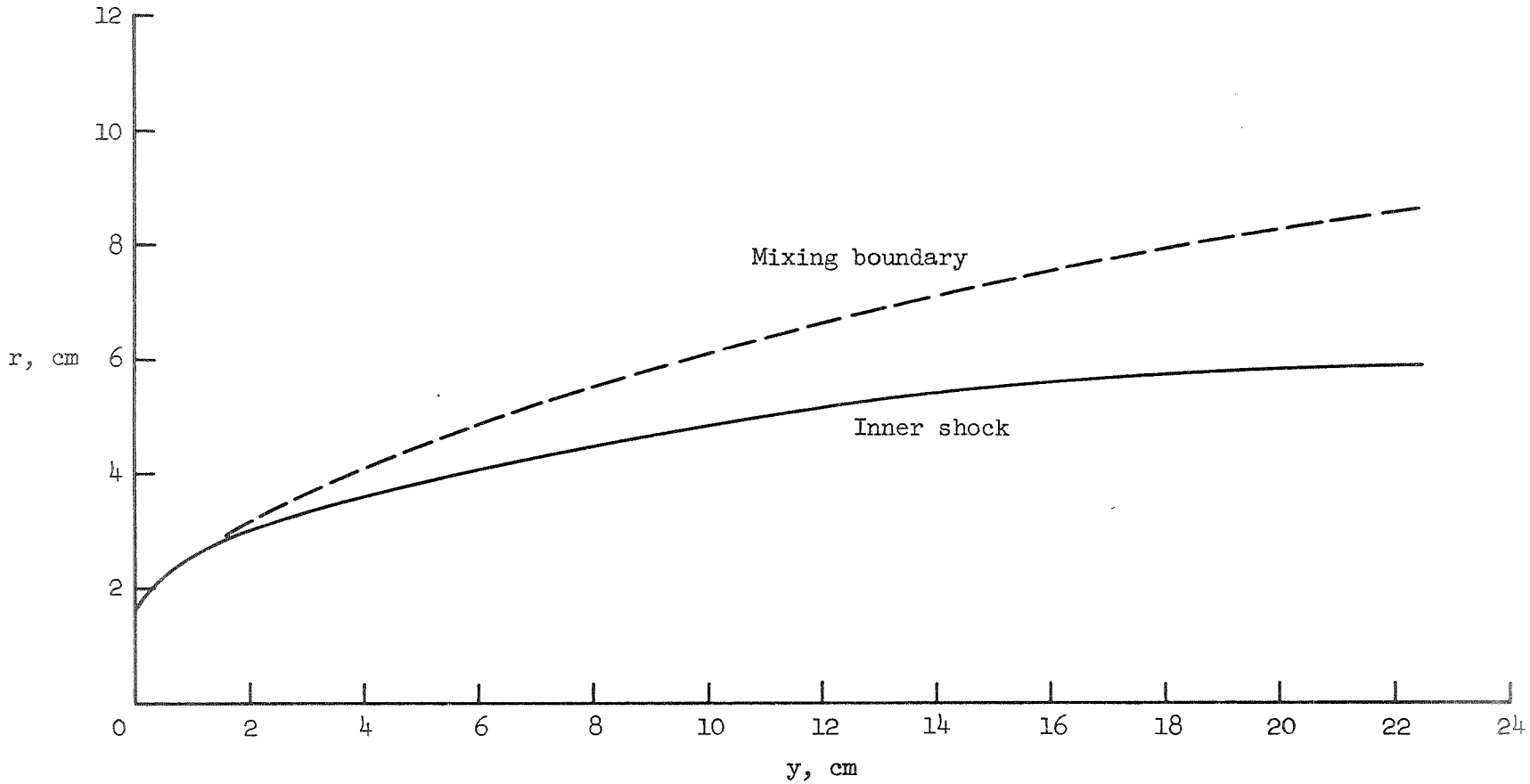

(a) M = 2.94

Figure 5.- Plume coordinates.

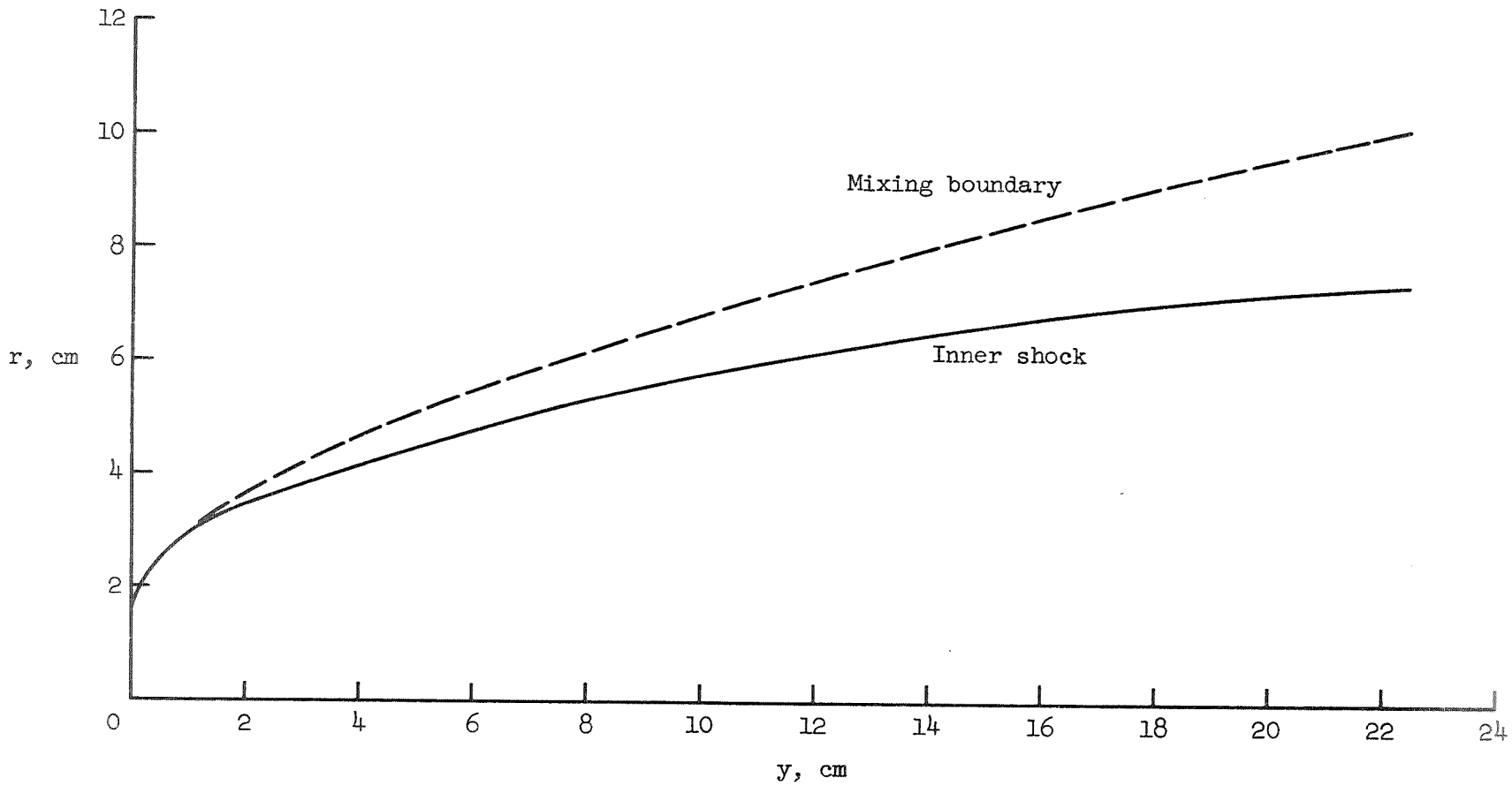

(b) M = 3.92

Figure 5.- Concluded.

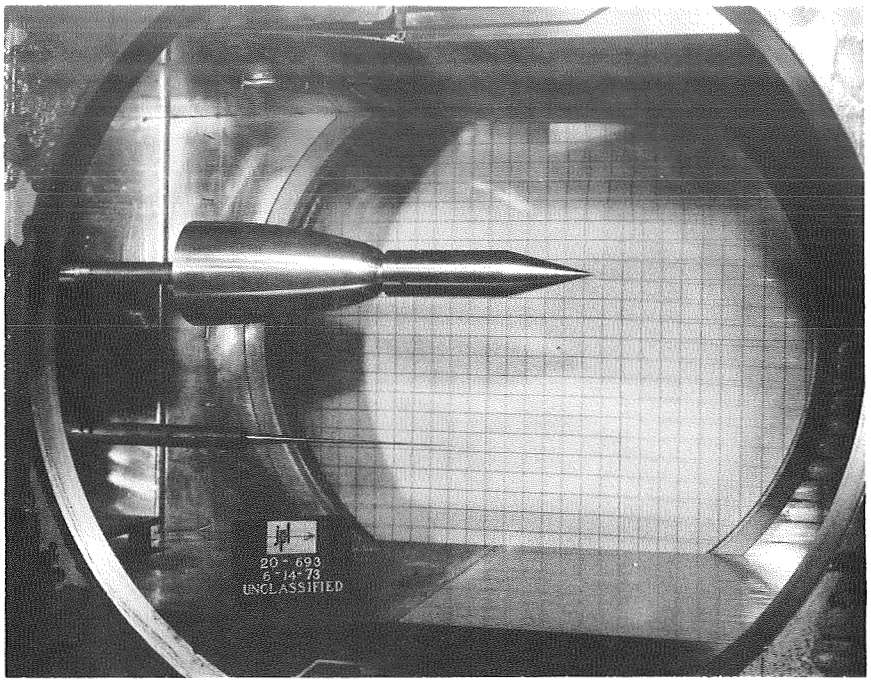

(a) Solid body plume sized by inner shock dimensions; M = 2.94.

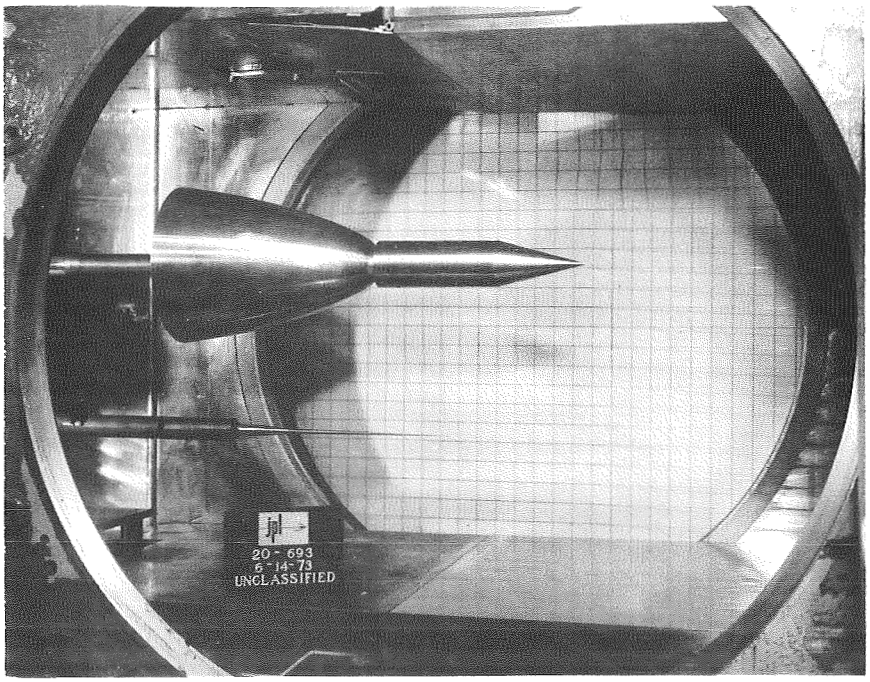

(b) Solid body plume sized by mixing boundary dimensions; M = 2.94.

Figure 6.- Photographs of cone-cylinder model with solid body exhaust plumes.

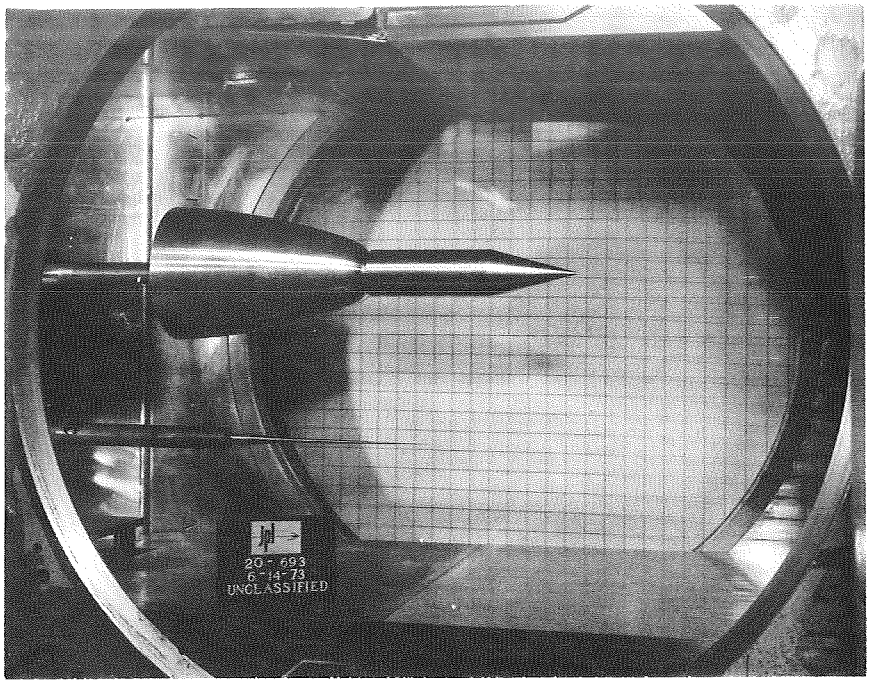

(c) Solid body plume sized by inner shock dimensions; M = 3.92.

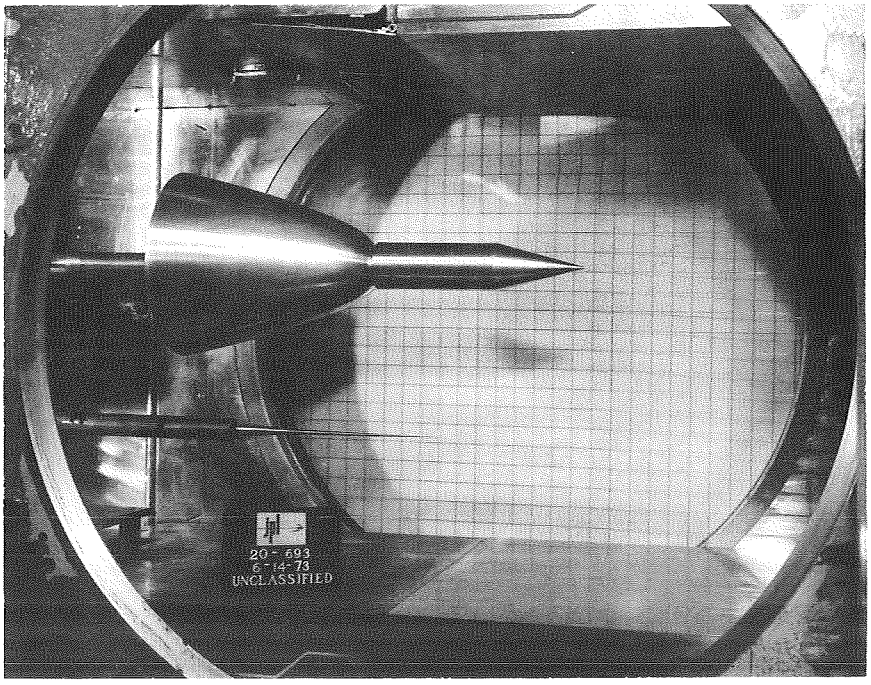

(d) Solid body plume sized by mixing boundary dimensions; M = 3.92.

Figure 6.- Concluded.

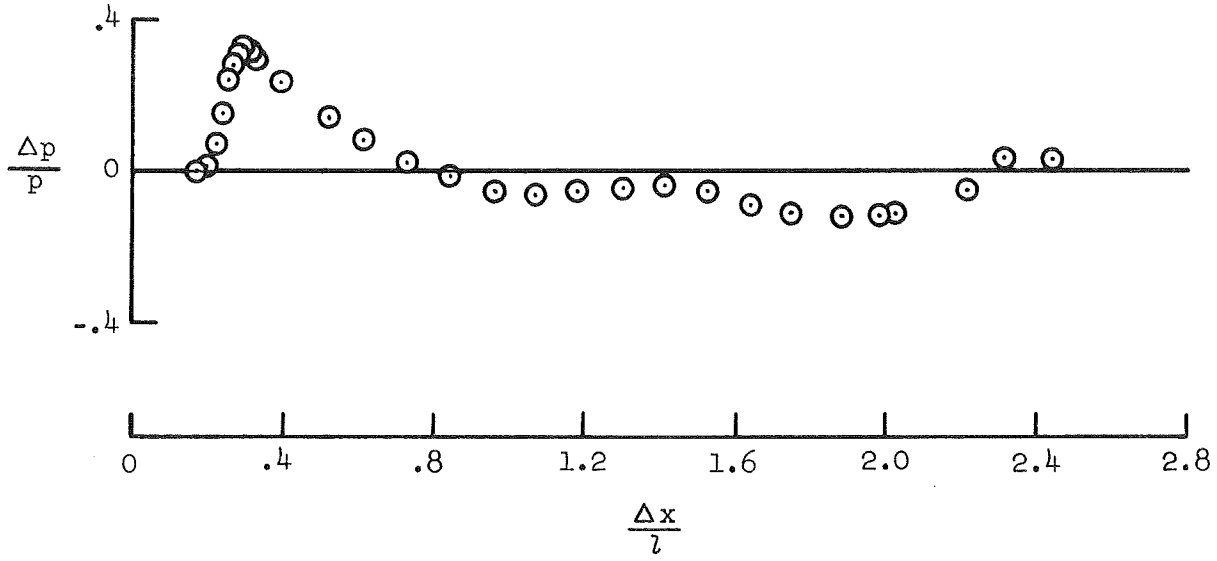

(a) No plume; M = 2.94.

Figure 7.- Wind tunnel pressure signatures generated by cone-cylinder model; $h/l = 0.819$.

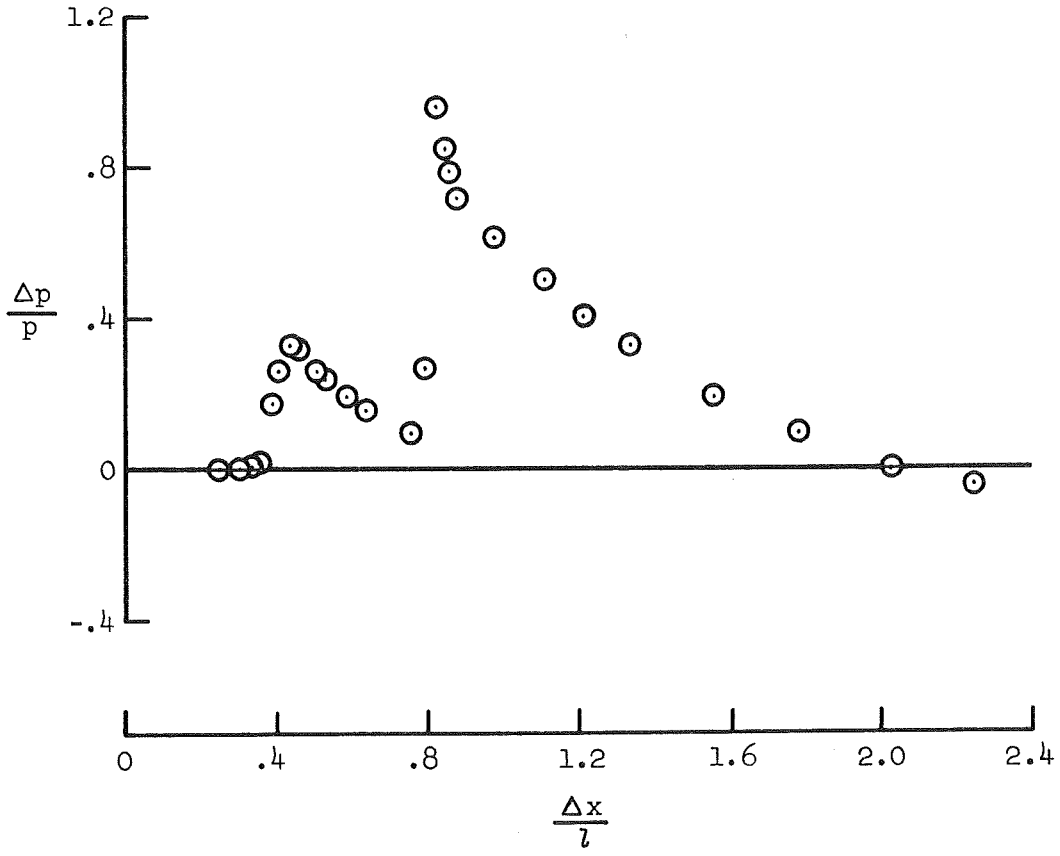

(b) Nitrogen plume; M = 2.94.

Figure 7.- Continued.

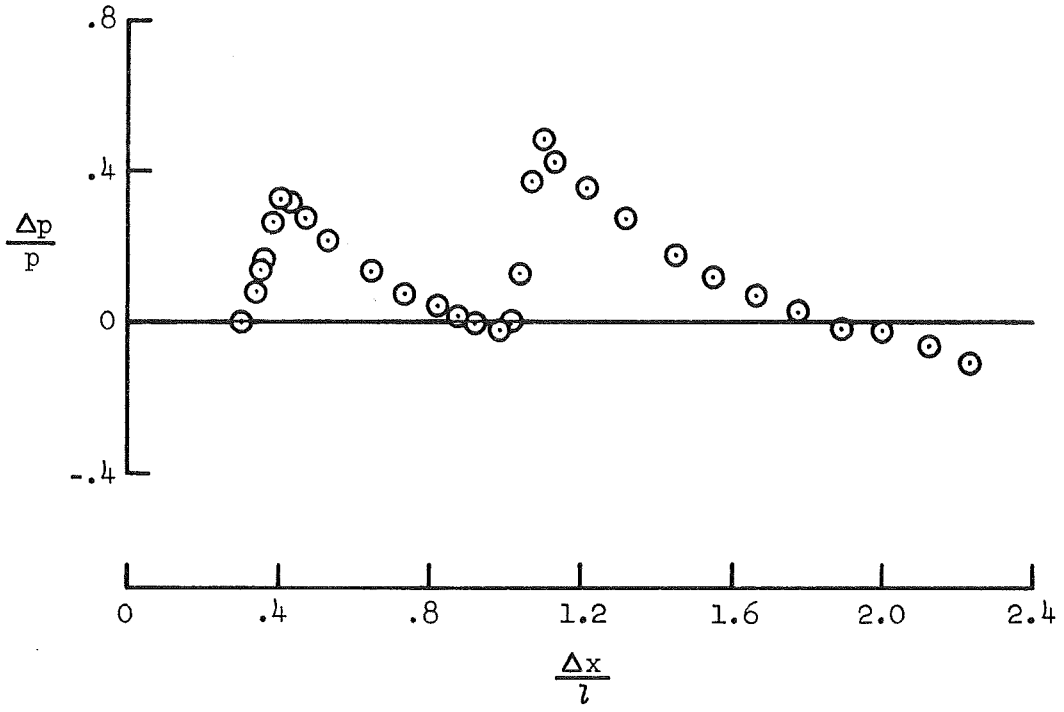

(c) Solid body plume sized by inner shock dimensions; M = 2.94.

Figure 7.- Continued.

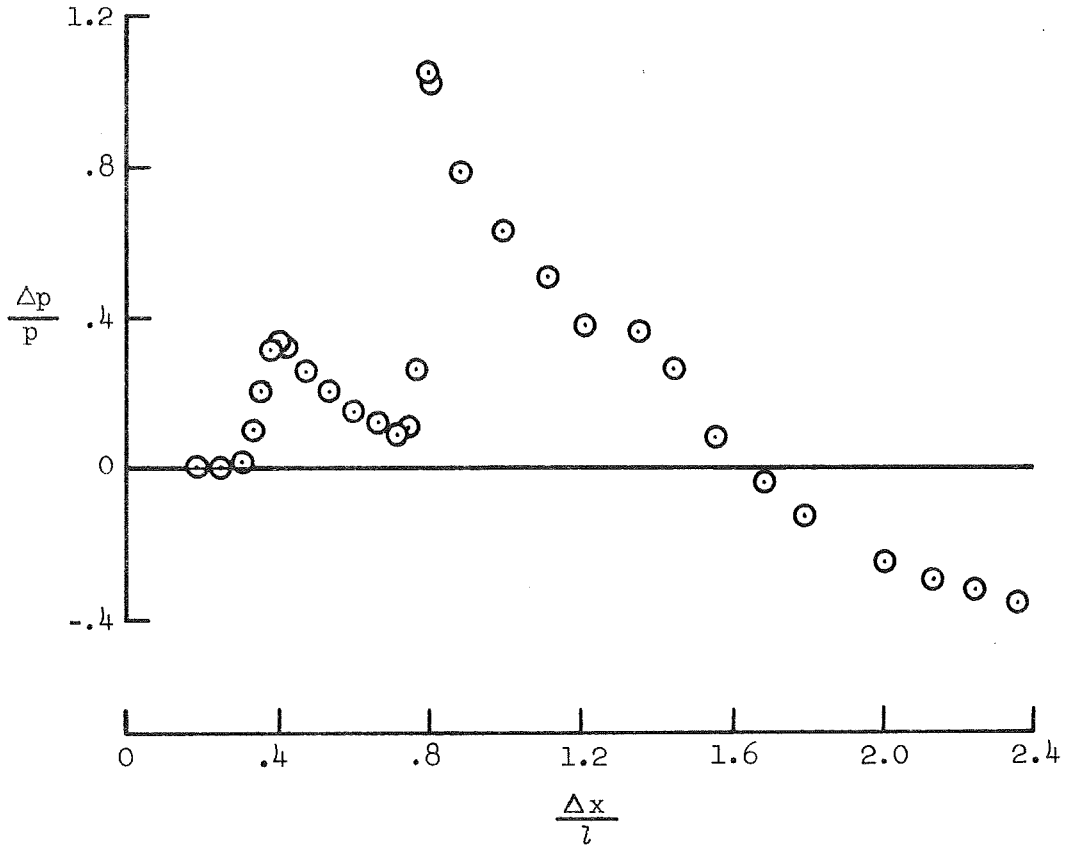

(d) Solid body plume sized by mixing boundary dimensions; M = 2.94.

Figure 7.- Continued.

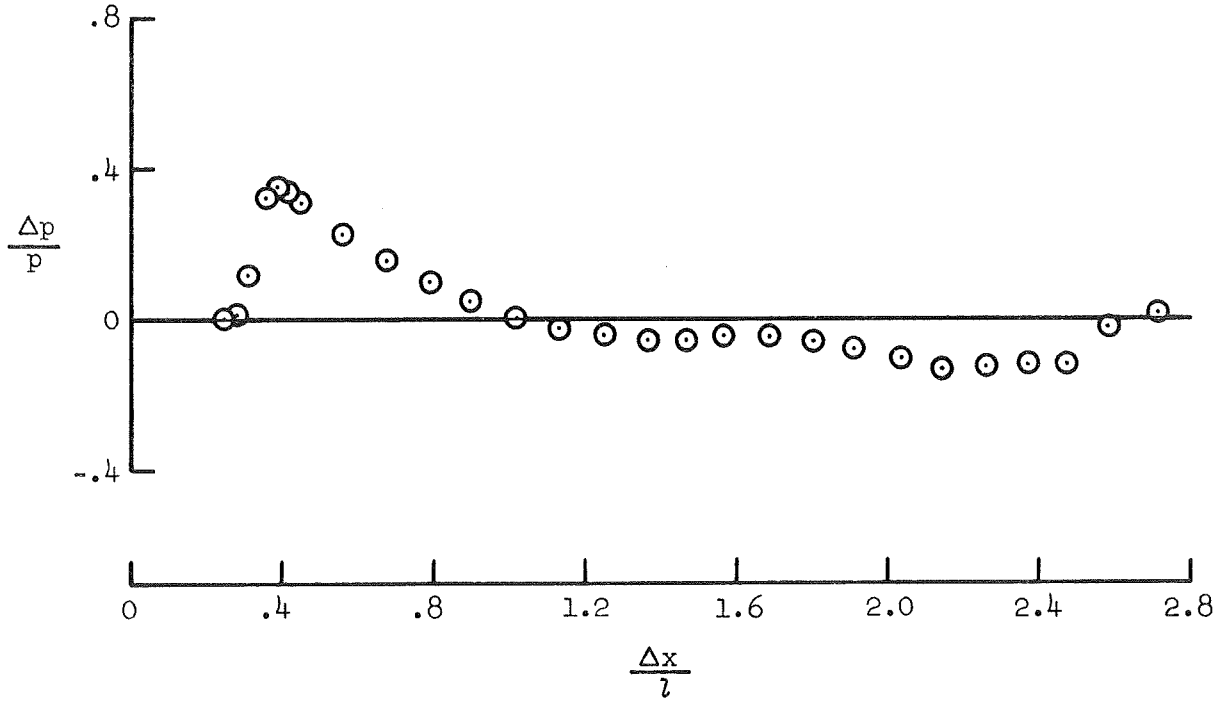

(e) No plume; M = 3.92.

Figure 7.- Continued.

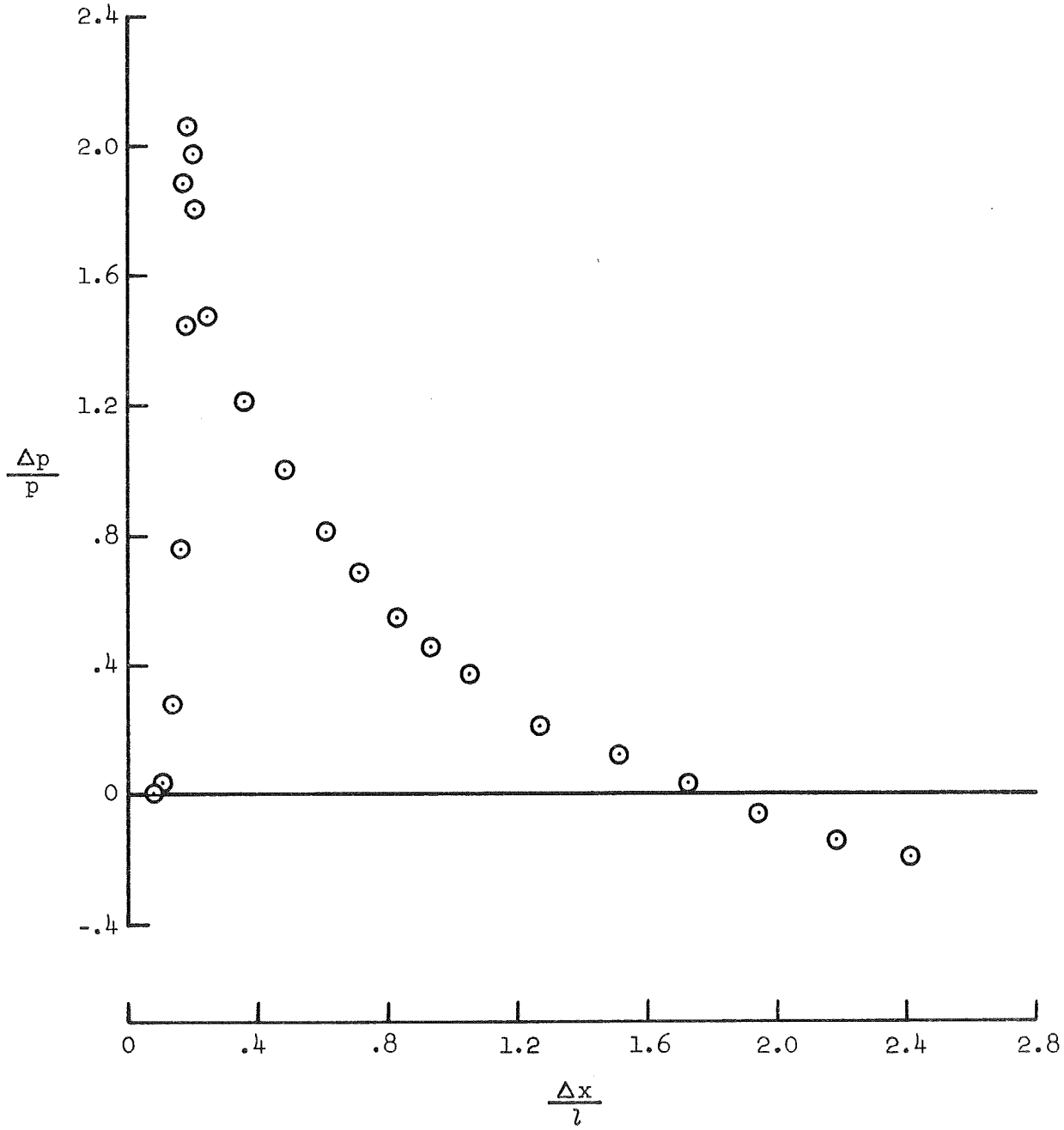

(f) Nitrogen plume; M = 3.92.

Figure 7.- Continued.

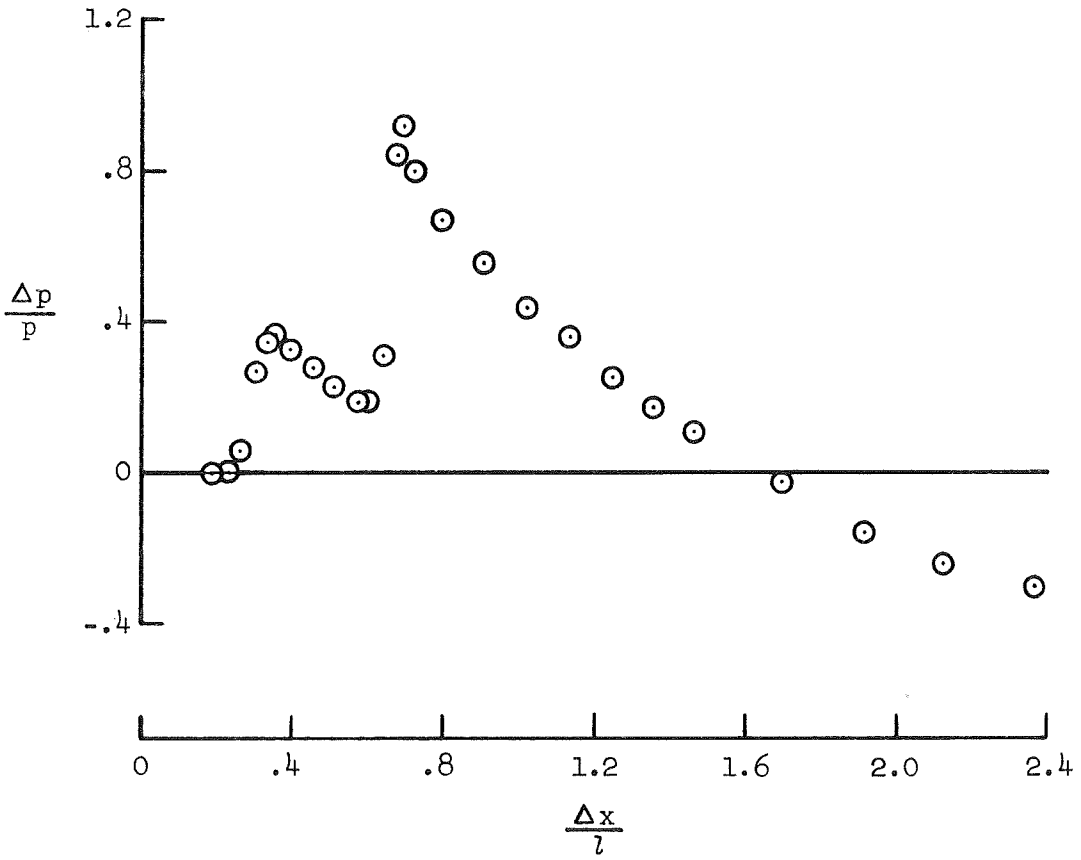

(g) Solid body plume sized by inner shock dimensions; M = 3.92.

Figure 7.- Continued.

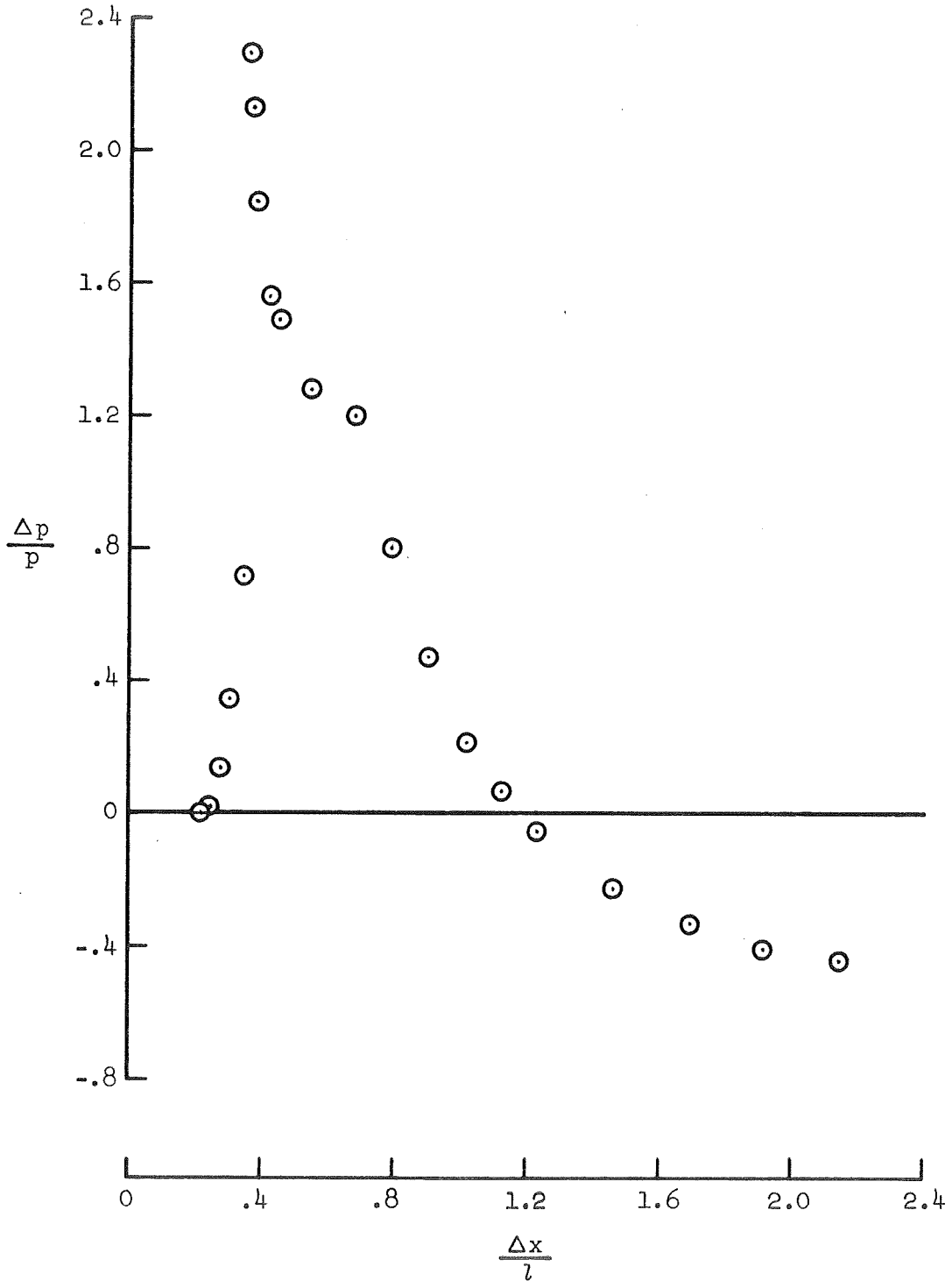

(h) Solid body plume sized by mixing boundary dimensions; M = 3.92.

Figure 7.- Concluded.

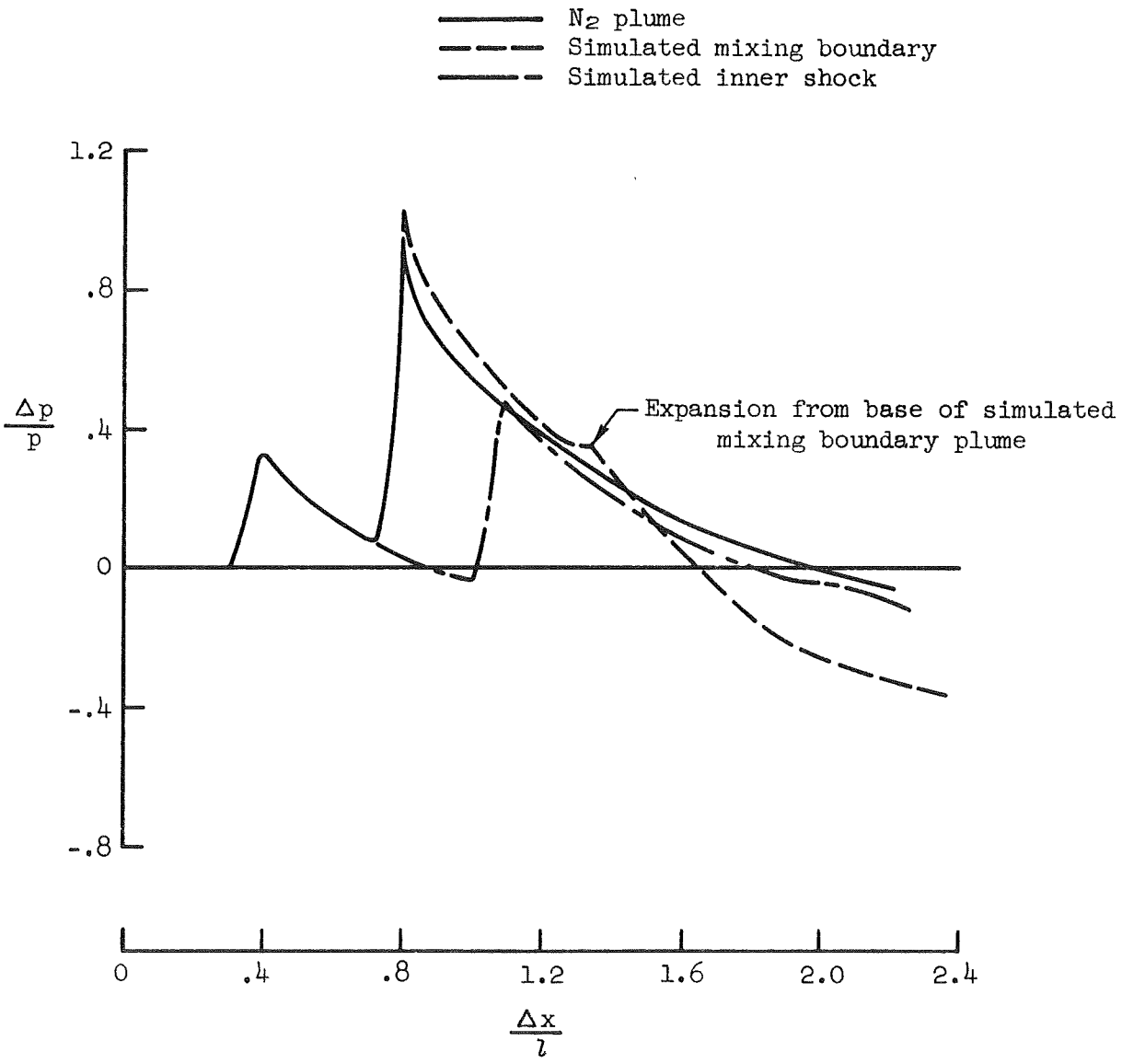

(a) M = 2.94

Figure 8.- Comparison of pressure signatures for nitrogen and solid body exhaust plumes; $h/l = 0.819$.

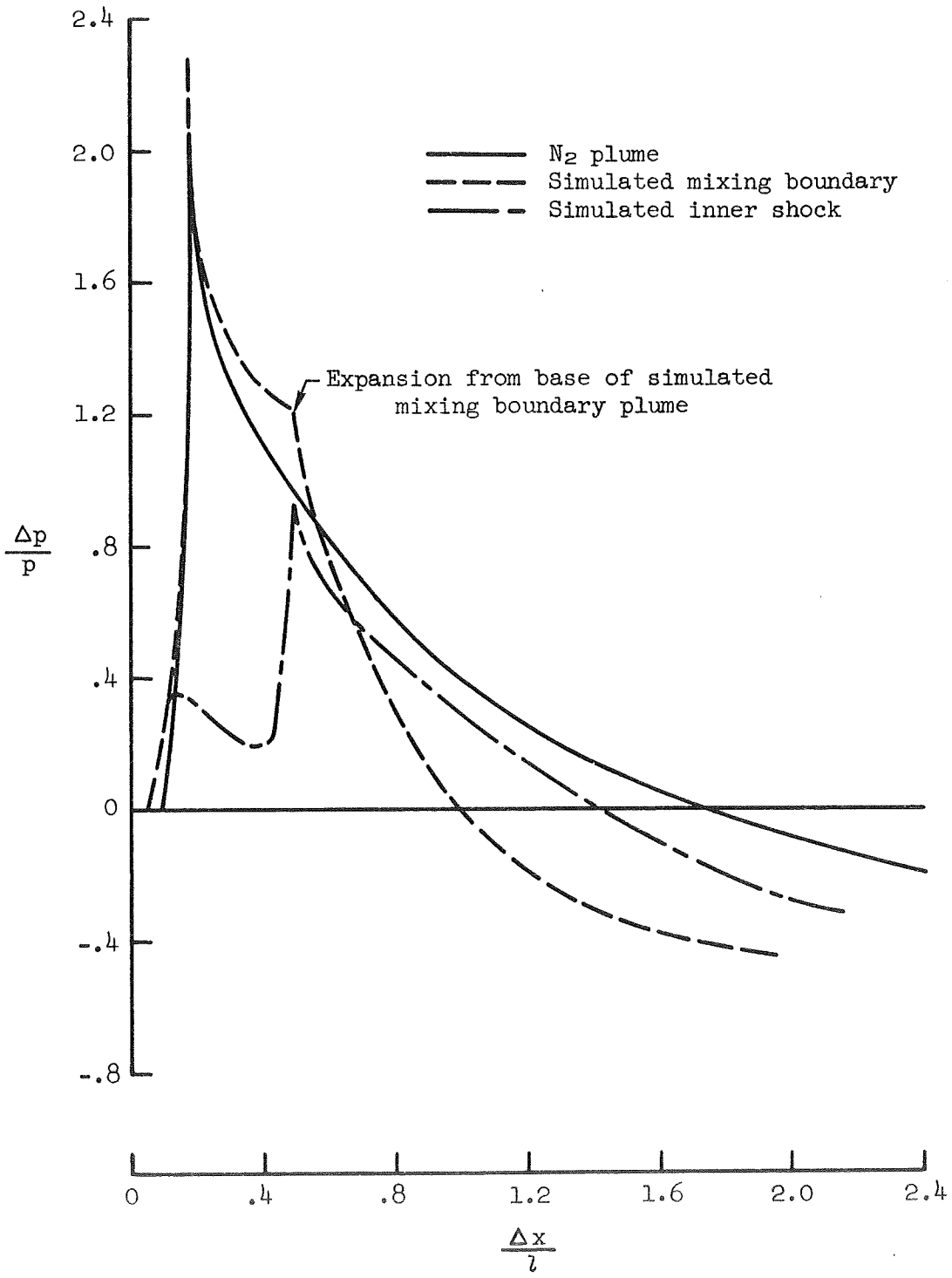

(b) M = 3.92

Figure 8.- Concluded.

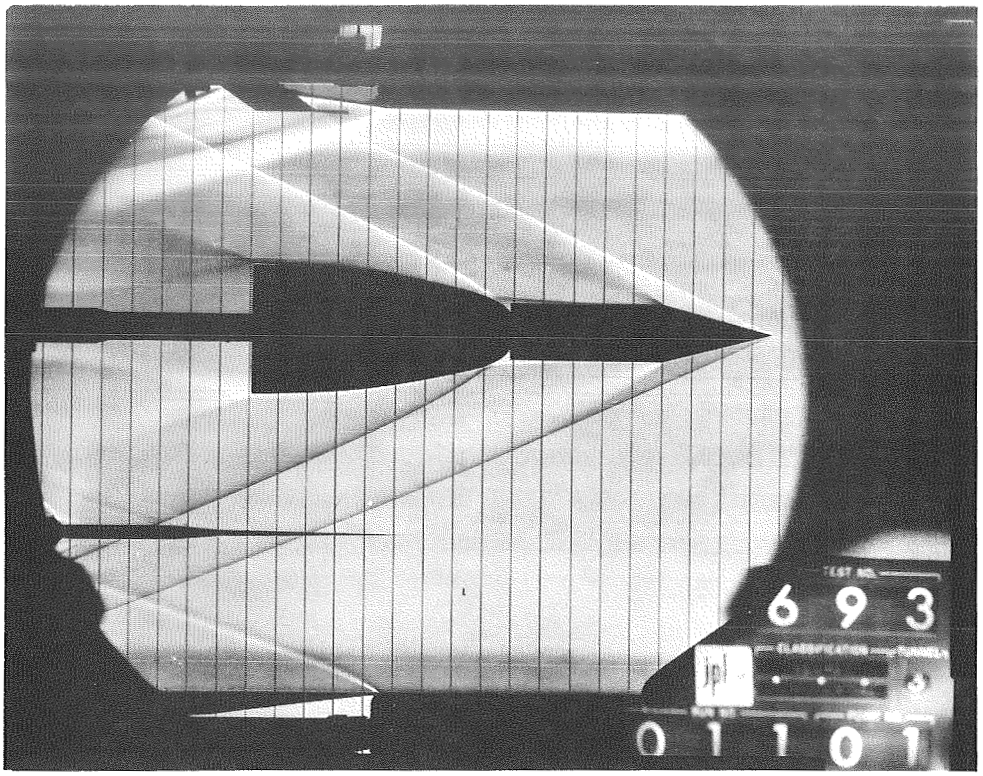

(a) Solid body plume sized by inner shock dimensions; M = 2.94.

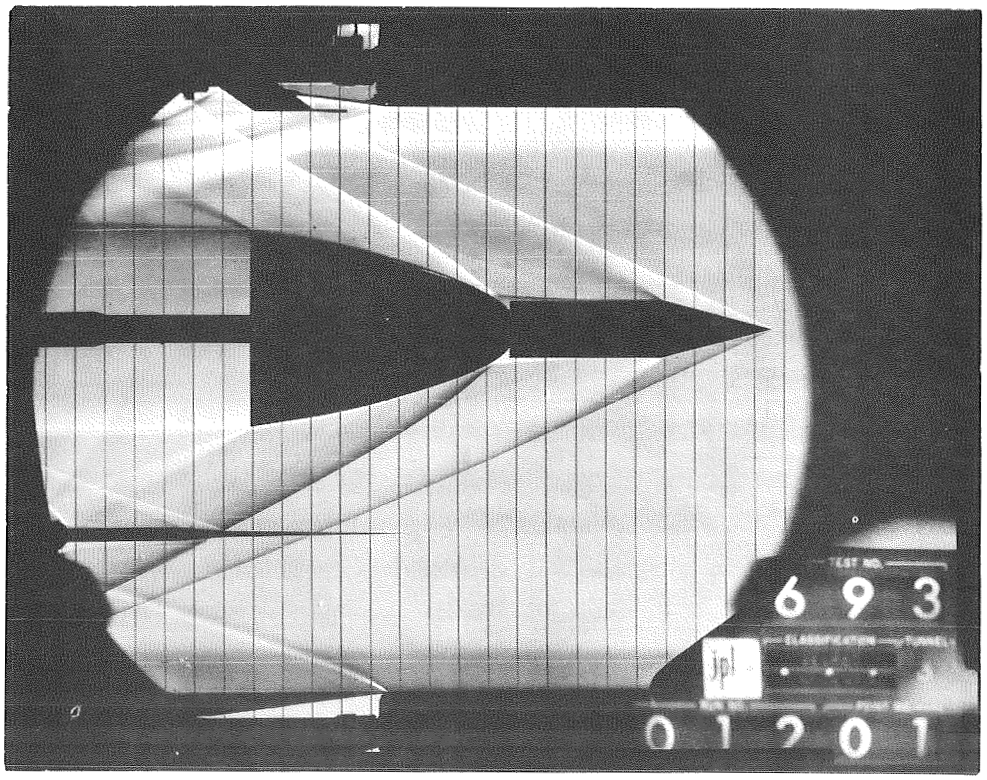

(b) Solid body plume sized by mixing boundary dimensions; M = 2.94.

Figure 9.- Schlieren photographs of cone-cylinder model with solid body exhaust plumes.

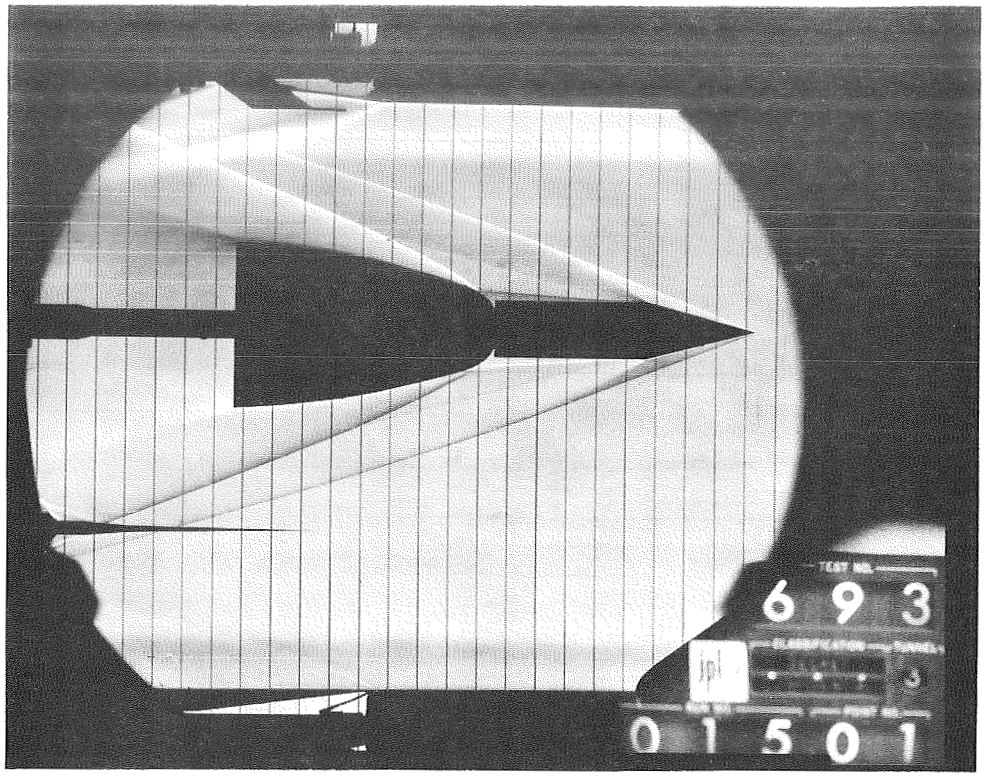

(c) Solid body plume sized by inner shock dimensions; M = 3.92.

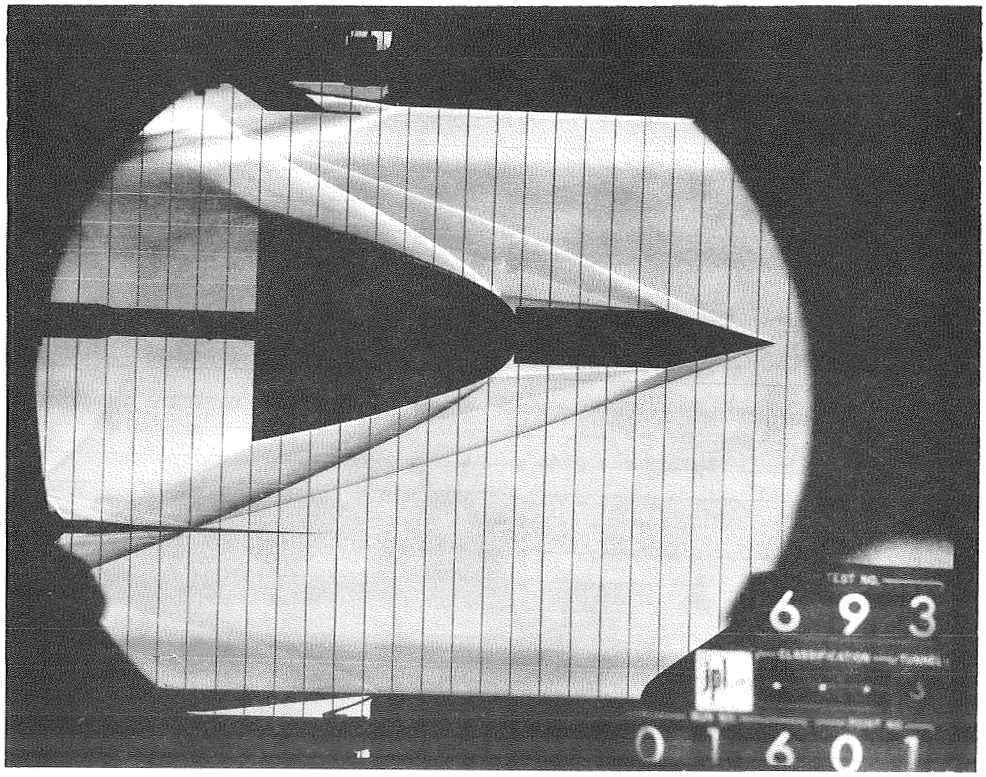

(d) Solid body plume sized by mixing boundary dimensions; M = 3.92.

Figure 9.- Concluded.

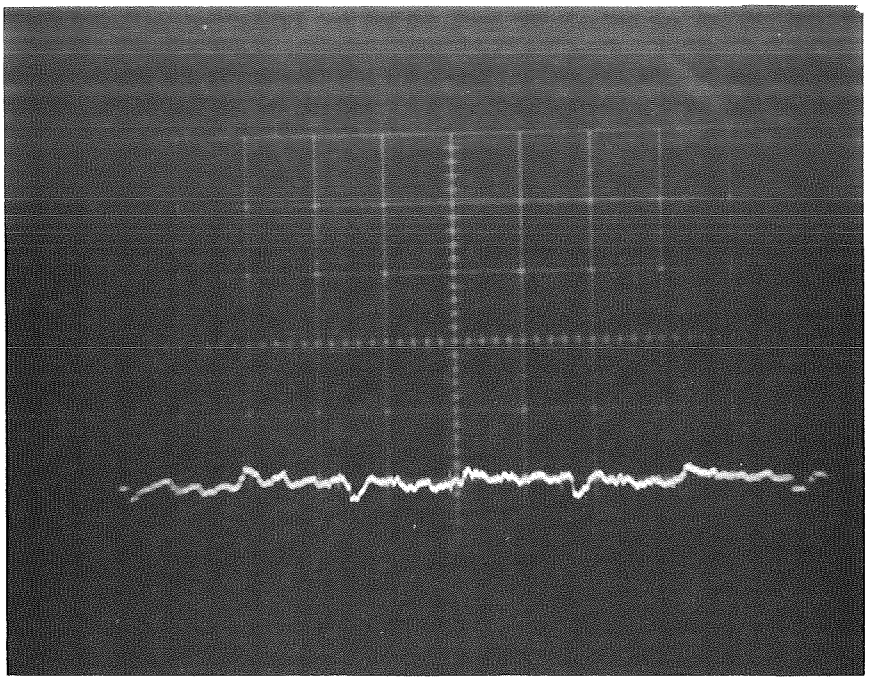

(a) Free stream; $\Delta x/l = 0.1$.

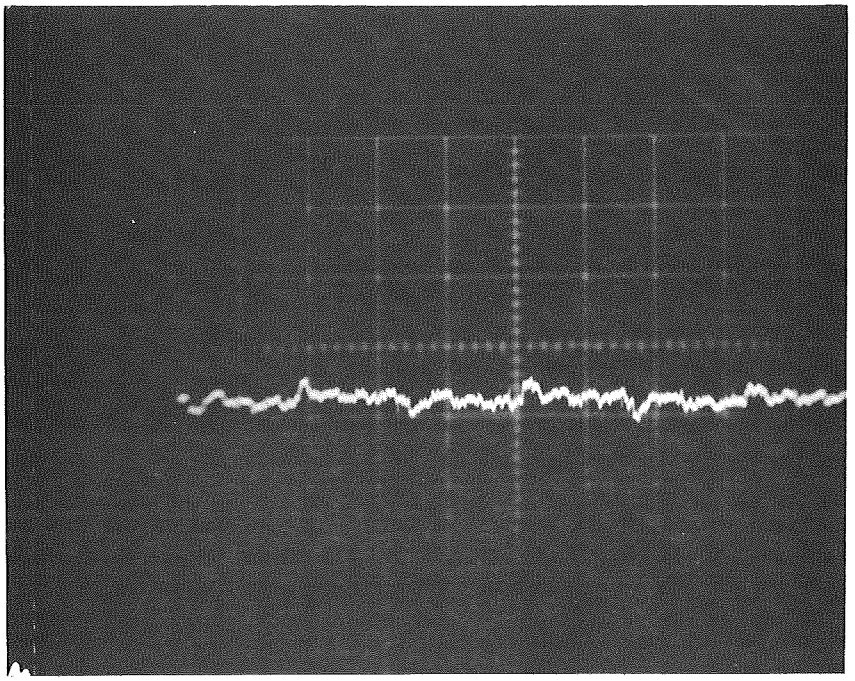

(b) Bow shock; $\Delta x/l = 0.3$.

Figure 10.- Oscilloscope records of flowfield pressures for cone-cylinder model with nitrogen plume; M = 2.94, $(\Delta p/p)/cm = 0.53$.

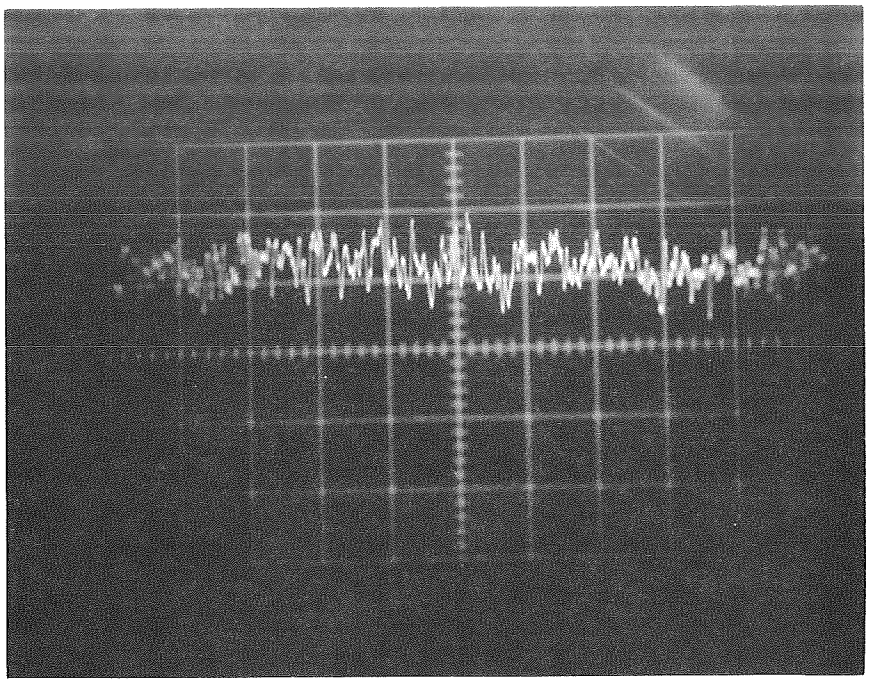

(c) Plume shock; $\Delta x/l = 0.79$.

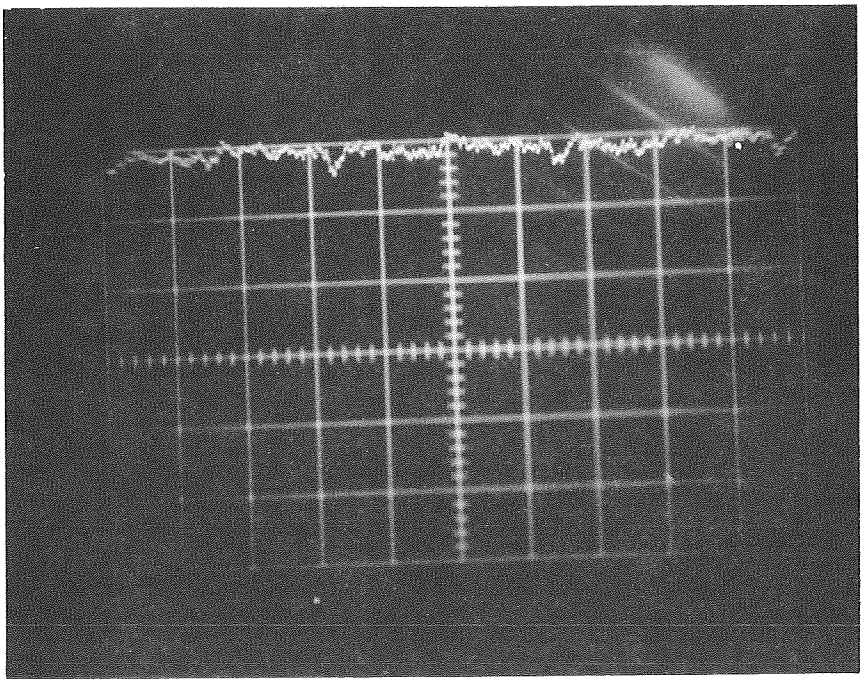

(d) Plume shock; $\Delta x/l = 0.82$.

Figure 10.- Continued.

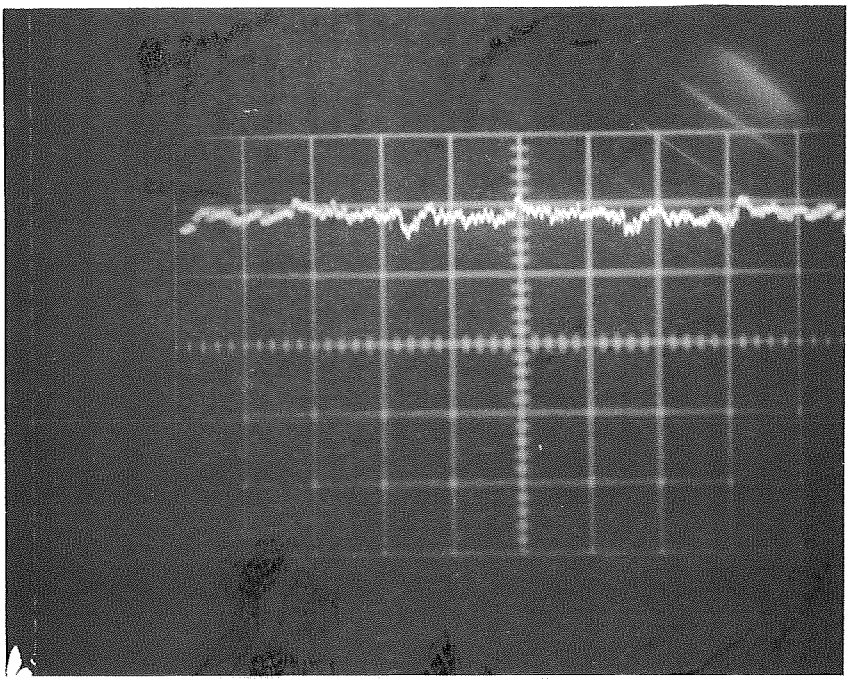

(e) Expansion behind plume shock; $\Delta x/l = 0.91$.

Figure 10.- Concluded.

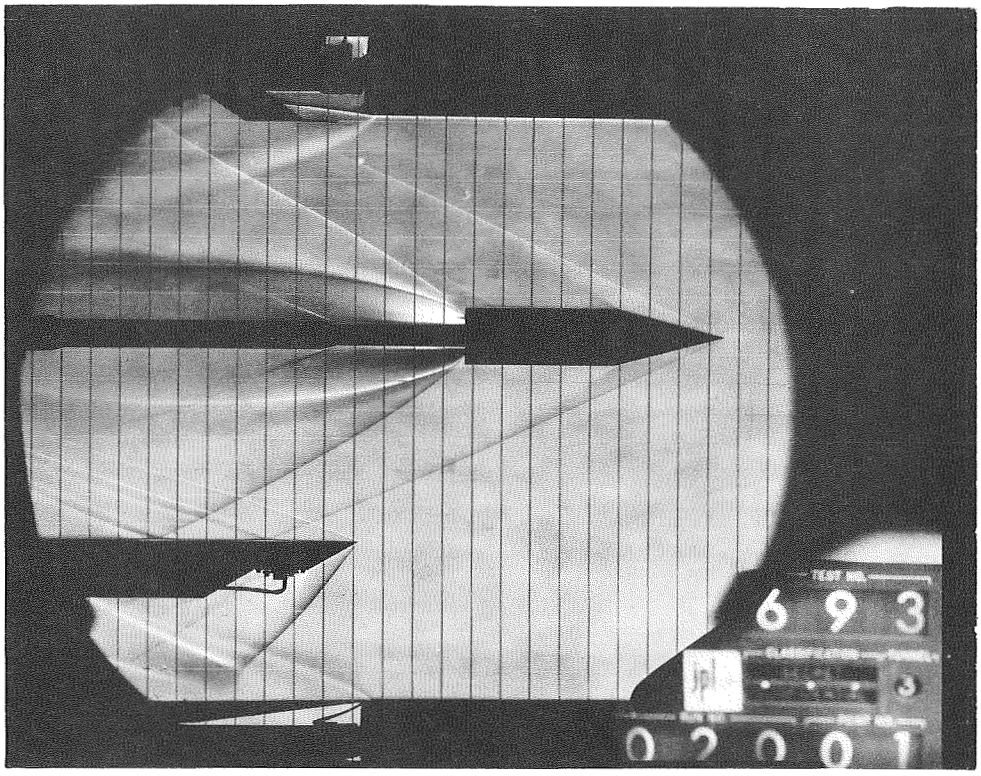

Figure 11.- Schlieren photograph showing shock induced boundary-layer separation on flat plate; M = 2.94.